Radiative Heat Transfer of a Two-Fluid Flow in a Vertical Porous Stratum[†]

J. C. Umavathi[1], **Ali J. Chamkha**[2], **M. H. Manjula**[1], and **A. Al-Mudhaf**[2]

[1]Department of Mathematics, Gulbarga University
Gulbarga, India

[2]Manufacturing Engineering Department,
The Public Authority for Applied Education and Training
Shuweikh, Kuwait

The effect of thermal radiation on mixed convection flow of two immiscible fluids in a vertical porous stratum is considered in the presence of a heat source or sink. The flow model is based on the Darcy – Lapwood – Brinkman equation. The general governing momentum and energy equations for the immiscible fluids are coupled and nonlinear and cannot be solved in closed form. However, approximate analytical solutions are obtained for small values of $\varepsilon = \Pr \mathrm{Ec}$ (the product of the Prandtl and Eckert numbers) using the regular perturbation method, while numerical solutions are found for large values of ε. A representation of the results is presented graphically to illustrate the influence of the physical parameters on the solutions. It is found that both the velocity and temperature fields can be controlled effectively by altering the values of the viscosity ratio, width ratio, and heat generation or absorption coefficient.

* * *

Nomenclature

b	ratio of the coefficients of thermal expansion $[\beta_2/\beta_1]$;
C_p	specific heat at constant pressure;
E^2	radiation parameter $[C(\alpha)h_1^2/K_1]$;
Ec	Eckert number $[\overline{u}_1^2/(C_p\Delta T)]$;
g	acceleration due to gravity;
Gr	Grashof number $[g\beta h_1^3\Delta T/\nu_1^2]$;
k	permeability of the porous medium;
K	thermal conductivity of the fluid-saturated porous medium;
P	nondimensional pressure gradient $[(h_1^2/\mu_1\overline{u}_1)\partial p/\partial x]$;

[†]Received 16.12.2007

ISSN 1064-2277

Pr	Prandtl number $[\mu_1 C_p/K_1]$;
Re	Reynolds number $[\overline{u}_1 h_1/\nu_1]$;
u	velocity;
$\overline{u}_1$	average velocity;
T	temperature;
T_W	wall temperature;
T_{W_0}	wall temperature at $y = 0$;
α	thermal diffusivity;
β	coefficient of thermal expansion;
σ	porous parameter $[h_1/\sqrt{k_1}]$;
ϕ	dimensionless heat generation or absorption coefficient $[\phi = Qh^2/K]$;
ρ_0	constant reference density;
ρ_i	density of the fluid;
ν	kinematic viscosity;
μ_i	viscosity;
ε	product of Prandtl and Eckert numbers [Pr Ec];
θ	nondimensional temperature $[(T - T_{W_2})/(T_{W_1} - T_{W_2})]$;
1, 2	quantities for regions I and II, respectively.

Introduction

Extensive reviews of prior work on convective flows in porous media have been presented by Combarnous & Bories [1], Cheng [2], Rudraiah [3, 4], Nield [5], Kaviany [6], and Nield and Bejan [7]. Most of the theoretical work has been based on Darcy's law, and as noted by Prasad et al. [8], the experimental results never agreed with the theoretical results obtained with the Darcy model. This has led to inclusion of inertia and viscous effects in studies of convection in porous media [4, 9–14]. Malashetty et al. [15] studied the convective flow and heat transfer in an inclined composite porous medium, using the Darcy – Lapwood – Brinkman equation.

Analysis of radioactive heat transfer with an absorbing-emitting media has received considerable attention due to its immense practical applications. Radiation heat transfer occurs when a sufficiently transparent continuous medium, such as air, separates the heat-exchanging surfaces, as in the case of most of the domestic and solar heating arrangements that surround us. Indeed, in many engineering problems, the challenge is to evaluate the total heat transfer rate when the radiation, convection and conduction mechanisms participate simultaneously [16]. The notable works incorporating the radiation effect in nonporous medium include convection of a radiation gas in a vertical channel [17, 18], heat transfer in an arbitrary medium [19], and transfer of heat in nongray gases [20, 21]. Recently, Chamkha [22] studied the effects of heat absorption and thermal radiation on heat transfer in a fluid-particle flow past a surface in the presence of a gravity field. Keeping in view the applications of multiphase flows through porous media and combined effect of natural convection and radiation as mentioned above, hence, it is the objective of this paper to consider the effect of radiation in a vertical channel of two immiscible fluids.

1. Mathematical Formulation

Consider the flow of two immiscible fluids in a saturated vertical porous medium bounded between two infinite parallel walls. The x-axis is taken along the walls and the y-axis is perpendicular

to it. The walls are placed at a distance 2h apart and are maintained at constant but different temperatures T_{W_1} and T_{W_2} in the presence of a gravity field, heat generation, or absorption and thermal radiation. The region $0 \geq y \geq h_1$ (region I) is filled with porous material having permeability k_1 and saturated with a fluid having a density ρ_1, dynamic viscosity μ_1, thermal conductivity K_1, and C_1 (a measure of energy transport due to radiation). The region $-h_2 \leq y \leq 0$ (region II) is filled with another porous material having permeability k_2 and saturated with another fluid having a density ρ_2, dynamic viscosity μ_2, thermal conductivity K_2, and C_2 (a measure of energy transport due to radiation.

The flow is assumed to be steady, laminar, and fully developed, and all fluid properties are constant except the density in the buoyancy terms of the momentum equations of both fluids. It is also assumed that at any given instant, the temperature of the fluid and the temperature of the solid in both regions are same. That is, in each region, both the fluid and the porous material are in local thermal equilibrium. The flow is assumed to be driven by a constant pressure gradient $(-\partial P/\partial x)$ and temperature gradient $\Delta T = T_{W_1} - T_{W_2}$. It should be mentioned that ΔT is positive, and the transport properties of both fluids are assumed to be constant.

The investigations on convection in a porous medium, discussed by many authors [23–26], are concerned with low-speed flows. It is well known that the flow of a fluid in a porous medium is curvilinear and the curvature of the path gives rise to inertial acceleration. Lapwood (1978) gave a systematic mathematical analysis to study linear convection in a porous medium using a generalized Darcy equation. The analysis of flow through a porous medium using the Lapwood – Darcy model [27–29] shows that the vorticity emerges at the discontinuity surface of permeability when the fluid flows across the surface and it decays steadily in the flow when the permeability is constant. To account for this decay, we must consider the viscous force. Recently, many authors [10, 30–34] have generalized Darcy equation, incorporating the inertial and viscous forces in addition to Darcy friction known as Darcy – Lapwood – Brinkman equation [4].

Under these assumptions, the governing equations of motion and energy for incompressible Boussinesq fluid (following [3, 4]) are as follows:

for phase I:

$$\mu_1 \frac{d^2u}{dy^2} + \rho_1 g \beta_1 (T_1 - T_{W_2}) - \frac{\mu_1 u_1}{k_1} = \frac{\partial P}{\partial x}, \tag{1}$$

$$\frac{d^2T}{dy^2} + \frac{\mu_1}{K_1}\left(\frac{du_1}{dy}\right)^2 + \frac{\mu_1}{K_1 k_1}u_1^2 - \frac{1}{K_1 \rho_0 C_p}\frac{\partial q_{R_1}}{\partial y} + \frac{Q_1}{K_1}(T_1 - T_{W_2}) = 0; \tag{2}$$

for phase II:

$$\mu_2 \frac{d^2u_2}{dy_2^2} + \rho_2 g \beta_2 (T_2 - T_{W_2}) - \frac{\mu_2}{k_2}u_2 = \frac{\partial P}{\partial x}, \tag{3}$$

$$\frac{d^2T_2}{dy^2} + \frac{\mu_2}{K_2}\left(\frac{du_2}{dy}\right)^2 + \frac{\mu_2}{K_2 k_2}u_2^2 - \frac{1}{K_2 \rho_0 C_p}\frac{\partial q_{R_2}}{\partial y} + \frac{Q_2}{K_2}(T_2 - T_{W_2}) = 0. \tag{4}$$

Here, u is the x-component of fluid velocity; T is the fluid temperature; g is the acceleration due to gravity; β is the coefficient of thermal expansion. Subscripts 1 and 2 denote the values for phases I and II, respectively. Cogley et al. [21] have shown that in the optimally thin limit for a nongray gas near equilibrium, the following relations hold:

$$\frac{\partial q_{R_1}}{\partial y} = 4\,(T_1 - T_{W_1}) \int_0^\infty K_{\lambda W}\left(\frac{de_{b\lambda}}{dT_W}\right) d\lambda, \tag{5}$$

$$\frac{\partial q_{R_2}}{\partial y} = 4\,(T_2 - T_{W_2}) \int_0^\infty K_{\lambda W} \left(\frac{de_{b\lambda}}{dT_W}\right) d\lambda, \tag{6}$$

where K_λ is the absorption coefficient; $e_{b\lambda}$ is the Plank function; the subscript W refers to values evaluated at the walls.

Using Eqs. (5) and (6) into Eqs. (2) and (4) gives

$$\frac{d^2T_1}{dy^2} + \frac{\mu_1}{K_1}\left(\frac{du_1}{dy}\right)^2 + \frac{\mu_1}{K_1 k_1}u_1^2 - C(\alpha)(T_1 - T_{W_2}) + \frac{Q_1}{K_1}(T_1 - T_{W_2}) = 0, \tag{7}$$

$$\frac{d^2T_2}{dy^2} + \frac{\mu_2}{K_2}\left(\frac{du_2}{dy}\right)^2 + \frac{\mu_2}{K_2 k_2}u_2^2 - C(\alpha)(T_2 - T_{W_2}) + \frac{Q_2}{K_2}(T_2 - T_{W_2}) = 0, \tag{8}$$

where

$$C(\alpha) = \frac{4}{\rho C_p} \int_0^\infty K_{\lambda_0} \left(\frac{de_{b\lambda}}{dT}\right)_0 d\lambda.$$

The subscript 0 indicates that all quantities have been evaluated at the reference temperature T_{W_0}, defined in the Nomenclature. The boundary conditions on velocity are no-slip conditions requiring that the velocity must vanish at the wall. The boundary condtions on temperature are isothermal conditions. The two boundaries are held at constant but different temperatures. In addition, the continuity of velocity, shear stress, temperature, and heat flux at the interface between the two porous layers is assumed.

The boundary and interface conditions on velocity are as follows:

$$\begin{gathered} u_1(h_1) = 0, \qquad u_1(0) = u_2(0), \qquad u_2(-h_2) = 0, \\ \mu_1 \frac{du_1}{dy_1} = \mu_2 \frac{du_2}{dy_2} \quad \text{at} \quad y = 0. \end{gathered} \tag{9}$$

The boundary and interface conditions for temperature are given by

$$\begin{gathered} T_1(h_1) = T_{W_1}, \qquad T_1(0) = T_2(0), \qquad T_2(-h_2) = T_{W_2}, \\ K_1 \frac{dT_1}{dy_1} = K_2 \frac{dT_2}{dy_2} \quad \text{at} \quad y = 0. \end{gathered} \tag{10}$$

Eqs. (1)–(8) along with boundary conditions Eqs. (9) and (10) are made dimensionless by using the following transformations:

$$\begin{gathered} u_1^* = \frac{u_1}{\overline{u}_1}, \qquad u_2^* = \frac{u_2}{\overline{u}_1}, \qquad y_1^* = \frac{y_1}{h_1}, \qquad y_2^* = \frac{y_2}{h_2}, \\ \theta = \frac{T - T_{W_2}}{\Delta T}, \qquad m = \frac{\mu_1}{\mu_2}, \qquad K = \frac{K_1}{K_2}, \qquad h = \frac{h_2}{h_1}, \\ n = \frac{\rho_2}{\rho_1}, \qquad b = \frac{\beta_2}{\beta_1}, \qquad k = \frac{k_1}{k_2}. \end{gathered} \tag{11}$$

By using Eqs. (11), the dimensionless governing equations become:

for phase I:

$$\frac{d^2u_1}{dy^2} + \frac{\mathrm{Gr}}{\mathrm{Re}}\,\theta_1 - \sigma^2 u_1 = P, \tag{12}$$

$$\frac{d^2\theta_1}{dy^2} + \mathrm{Ec}\,\mathrm{Pr}\left(\frac{du_1}{dy}\right)^2 + \mathrm{Ec}\,\mathrm{Pr}\,\sigma^2 u_1^2 - E^2\theta_1 \pm \phi_1\theta_1 = 0; \tag{13}$$

for phase II:

$$\frac{d^2u_2}{dy^2} + \frac{\mathrm{Gr}}{\mathrm{Re}} b\,m\,n\,h^2\theta_2 - \sigma^2 h^2 k\,u_2 = m\,h^2 P, \tag{14}$$

$$\frac{d^2\theta_2}{dy^2} + \frac{\mathrm{Ec}\,\mathrm{Pr}\,K}{m}\left(\frac{du_2}{dy}\right)^2 + \mathrm{Ec}\,\mathrm{Pr}\,K h^2\sigma^2\frac{k}{m}u_2^2 - E^2h^2K\theta_2 \pm \phi_2\theta_2 = 0, \tag{15}$$

where

$$\mathrm{Gr} = \frac{g\beta_1 h_1^3\Delta T}{\nu_1^2}, \qquad \sigma = \frac{h_1}{\sqrt{k_1}}, \qquad \mathrm{Re} = \frac{\overline{u}_1\,h_1}{\nu_1},$$
$$\mathrm{Pr} = \frac{\mu_1 C_p}{K_1}, \qquad \mathrm{Ec} = \frac{(\overline{u}_1)^2}{C_p\Delta T}, \qquad P = \frac{h_1^2(\partial P/\partial x)}{\mu_1\overline{u}_1}.$$

The dimensionless form of the hydrodynamic and thermal boundary and interface conditions (9) and (10) become

$$\begin{gathered} u_1(1) = 0, \qquad u_1(0) = u_2(0), \qquad u_2(-1) = 0, \\ \frac{du_1}{dy} = \frac{1}{mh}\frac{du_2}{dy} \quad \text{at} \quad y = 0; \end{gathered} \tag{16}$$

$$\begin{gathered} \theta_1(0) = 1, \qquad \theta_1(0) = \theta_2(0), \qquad \theta_2(-1) = 0, \\ \frac{d\theta_1}{dy} = \frac{1}{K_1 h}\frac{d\theta_2}{dy} \quad \text{at} \quad y = 0. \end{gathered} \tag{17}$$

The asterisks have been dropped for simplicity.

2. Solutions

The governing momentum Eqs. (12) and (14), along with the energy Eqs. (13) and (15), are solved subject to the boundary and interface conditions Eqs. (16) and (17) for the velocity and temperature distributions. In this case, the equations are coupled through the buoyancy force and nonlinear due to the inclusion of the dissipation terms in the energy equation. In most practical problems, Ec is very small and is of order 10^{-5}. Thus, the fact that the product $\varepsilon = \mathrm{Pr}\,\mathrm{Ec}$ is very small can be exploited to use the regular perturbation method. To this end, the solutions are assumed in the following form:

$$(u_i, \theta_i) = (u_{i0}, \theta_{i0}) + \varepsilon(u_{i1}, \theta_{i1}) + \cdots, \tag{18}$$

where $i = 1, 2$, u_{i0} and θ_{i0} are solutions for the case in which ε equals to zero; u_{i1} and θ_{i1} are perturbed quantities relating to u_{i0}, θ_{i0}, respectively.

Substituting the above identities into Eqs. (12) – (15) and equating the coefficients of like powers of ε to zero, we obtain the zeroth- and first-order equations as follows:

for phase I:

- zeroth-order equations

$$\frac{d^2u_{10}}{dy^2} + \frac{\mathrm{Gr}}{\mathrm{Re}}\theta_{10} - \sigma^2 u_{10} = P, \tag{19}$$

$$\frac{d^2\theta_{10}}{dy^2} \pm \phi_1\,\theta_{10} - E^2\theta_{10} = 0; \tag{20}$$

- first-order equations

$$\frac{d^2u_{11}}{dy^2} + \frac{\mathrm{Gr}}{\mathrm{Re}}\theta_{11} - \sigma^2 u_{11} = 0, \tag{21}$$

$$\frac{d^2\theta_{11}}{dy^2} + \left(\frac{du_{10}}{dy}\right)^2 + \sigma^2 u_{10} \pm \phi_1\,\theta_{11} - E^2\theta_{11} = 0. \tag{22}$$

for phase II:

- zeroth-order equations

$$\frac{d^2u_{20}}{dy^2} + \frac{\mathrm{Gr}}{\mathrm{Re}}bmnh^2\theta_{20} - \sigma^2h^2ku_{20} = mh^2P, \tag{23}$$

$$\frac{d^2\theta_{20}}{dy^2} \pm \phi_2\theta_{20} - E^2h^2K\theta_{20} = 0; \tag{24}$$

- first-order equations

$$\frac{d^2u_{21}}{dy^2} + \frac{\mathrm{Gr}}{\mathrm{Re}}bmnh^2\theta_{21} - \sigma^2h^2ku_{21} = 0, \tag{25}$$

$$\frac{d^2\theta_{21}}{dy^2} + \frac{K}{m}\left(\frac{du_{20}}{dy}\right)^2 + Kh^2\sigma^2\frac{k}{m}u_{20}^2 - E^2h^2K\theta_{21} \pm \phi_2\theta_{21} = 0. \tag{26}$$

The corresponding boundary and interface conditions Eqs. (16) and (17) reduce to the following:

- zeroth-order conditions

$$\begin{gathered} u_{10}(1) = 0, \qquad u_{10}(0) = u_{20}(0), \qquad u_{20}(-1) = 0, \\ \frac{du_{10}}{dy} = \frac{1}{mh}\frac{du_{20}}{dy} \quad \text{at} \quad y = 0, \end{gathered} \tag{27}$$

$$\begin{gathered} \theta_{10}(1) = 1, \qquad \theta_{10}(0) = \theta_{20}(0), \qquad \theta_{20}(-1) = 0, \\ \frac{d\theta_{10}}{dy} = \frac{1}{Kh}\frac{d\theta_{20}}{dy} \quad \text{at} \quad y = 0; \end{gathered} \tag{28}$$

- first-order conditions

$$u_{11}(1) = 0, \qquad u_{11}(0) = u_{21}(0), \qquad u_{21}(-1) = 0,$$
$$\frac{du_{11}}{dy} = \frac{1}{mh}\frac{du_{21}}{dy} \quad \text{at} \quad y = 0, \tag{29}$$

$$\theta_{11}(1) = 0 \qquad \theta_{11}(0) = \theta_{21}(0) \qquad \theta_{21}(-1) = 0$$
$$\frac{d\theta_{11}}{dy} = \frac{1}{Kh}\frac{d\theta_{21}}{dy} \quad \text{at} \quad y = 0. \tag{30}$$

Analytical solutions to Eqs. (19) – (26) subject to the boundary and interface conditions Eqs. (27) – (30) are found and given below. In this case, the equations are coupled and linear and, hence, closed-form solutions are possible. The form of the solutions for θ_1 and θ_2 is different, depending whether the signs before ϕ_1 and ϕ_2 in the energy equations are positive or negative. Therefore, two different solutions for θ_1 and θ_2 corresponding to the cases of heat-generating fluids ($\phi_1 > 0$, $\phi_2 > 0$) and heat-absorbing fluids ($-\phi_1 < 0$, $-\phi_2 < 0$) are obtained. Obviously, cases where one of the fluids is heat generating while the other is heat absorbing can be obtained in the same manner. For brevity, these cases will not be considered herein.

2.1. Heat generation case ($\boldsymbol{\phi_1 > 0}$, $\boldsymbol{\phi_2 > 0}$). Without going into detail, solution of the zeroth-order equations (19), (20), (23), (24) using boundary and interface conditions (27), (28) can be shown to be

$$\theta_{10} = B_1 \cos\sqrt{\phi_1 - E^2}y + B_2 \sin\sqrt{\phi_1 - E^2}y\,, \tag{31}$$

$$\theta_{20} = B_3 \cos\sqrt{\phi_2 - A_5}y + b_4 \sin\sqrt{\phi_2 - A_5}y\,, \tag{32}$$

$$u_{10} = B_5 e^{\sigma y} + B_5 e^{-\sigma y} + l_1 \cos\sqrt{\phi_1 - E^2}y + l_2 \sin\sqrt{\phi_1 - E^2}y + l_3, \tag{33}$$

$$u_{20} = B_7 e^{\sqrt{A_3}y} + B_8 e^{-\sqrt{A_3}y} + l_4 \cos\sqrt{\phi_2 - A_5}y + l_5 \sin\sqrt{\phi_2 - A_5}y + l_6. \tag{34}$$

The solutions of the first-order perturbation equations Eqs. (21), (22), (25) and (26) using boundary and interface conditions Eqs. (29), (30) are given by

$$\begin{aligned}\theta_{11} = \;& B_9 \cos P_1 y + B_{10} \sin P_1 y + r_{14} \cos 2P_1 y + r_{15} \sin 2P_1 y \\ & + r_{16} e^{\sigma y} \cos P_1 y + r_{17} e^{\sigma y} \sin P_1 y + r_{18} e^{-\sigma y} \cos P_1 y \\ & + r_{19} e^{-\sigma y} \sin P_1 y + r_{20} y \cos P_1 y + r_{21} y \sin P_1 y + r_{22} e^{2\sigma y} \\ & + r_{23} e^{-2\sigma y} + r_{24} e^{\sigma y} + r_{25} e^{-\sigma y} + r_{26},\end{aligned} \tag{35}$$

$$\begin{aligned}\theta_{21} = \;& B_{11} \cos P_2 y + B_{12} \sin P_2 y + g_{14} \cos 2P_2 y + g_{15} \sin 2P_2 y \\ & + g_{16} e^{\sqrt{A_3}y} \cos P_2 y + g_{17} e^{\sqrt{A_3}y} \sin P_2 y + g_{18} e^{-\sqrt{A_3}y} \cos P_2 y \\ & + g_{19} e^{-\sqrt{A_3}y} \sin P_2 y + g_{20} y \cos P_2 y + g_{21} y \sin P_2 y + g_{22} e^{2\sqrt{A_3}y} \\ & + g_{23} e^{-2\sqrt{A_3}y} + g_{24} e^{\sqrt{A_3}y} + g_{25} e^{-\sqrt{A_3}y} + g_{26},\end{aligned} \tag{36}$$

$$
\begin{aligned}
u_{11} = \; & B_{13}e^{\sigma\, y} + B_{14}e^{-\sigma\, y} + l_7 \cos 2P_1 y + l_8 \sin 2P_1 y + l_9 \cos 2P_1 y + l_{10} \sin 2P_1 y \\
& + l_{11} e^{\sigma\, y} \cos P_1 y + l_{12} e^{\sigma\, y} \sin P_1 y + l_{13} e^{-\sigma\, y} \cos P_1 y + l_{14} e^{-\sigma\, y} \sin P_1 y \\
& + l_{15} y \cos P_1 y + l_{16} y \sin P_1 y + l_{17} y e^{\sigma\, y} + l_{18} y e^{-\sigma\, y} + l_{19} e^{2\sigma\, y} + l_{20} e^{-2\sigma\, y} \\
& + l_{21},
\end{aligned} \tag{37}
$$

$$
\begin{aligned}
u_{21} = \; & B_{15}e^{\sqrt{A_3}y} + B_{16}e^{-\sqrt{A_3}y} + l_{22} \cos 2P_2 y + l_{23} \sin 2P_2 y + l_{24} \cos P_2 y \\
& + l_{25} \sin P_2 y + l_{26} e^{\sqrt{A_3}y} \cos P_2 y + l_{27} e^{\sqrt{A_3}y} \sin P_2 y + l_{28} e^{-\sqrt{A_3}y} \cos P_2 y \\
& + l_{29} e^{-\sqrt{A_3}y} \sin P_2 y + l_{30} y \cos P_2 y + l_{31} y \sin P_2 y + l_{32} e^{2\sqrt{A_3}y} + l_{33} e^{-2\sqrt{A_3}y} \\
& + l_{34} y e^{\sqrt{A_3}y} + l_{35} y e^{-\sqrt{A_3}y} + l_{36}.
\end{aligned} \tag{38}
$$

It should be noted that all of the constants appearing in the above solutions for the heat generation case are defined and given in the Appendix.

2.2. Heat absorption case($\phi_1 < 0$, $\phi_2 < 0$). In a similar fashion as in the case of heat generation, the solutions for this case can be obtained. Solutions of the zeroth-order equations (19), (20), (23), (24) using boundary and interface conditions (27), (28) can be written as

$$
\theta_{10} = B_1 \cosh \sqrt{\phi_1 + E^2}\, y + B_2 \sinh \sqrt{\phi_1 + E^2}\, y\,, \tag{39}
$$

$$
\theta_{20} = B_3 \cosh \sqrt{\phi_2 + A_5}\, y + B_4 \sinh \sqrt{\phi_2 + A_5}\, y\,, \tag{40}
$$

$$
u_{10} = B_5 \cosh \sigma\, y + B_6 \sinh \sigma\, y + l_1 \cosh \sqrt{\phi_1 + E^2}\, y + l_2 \sinh \sqrt{\phi_1 + E^2}\, y + l_3, \tag{41}
$$

$$
u_{20} = B_7 \cosh \sqrt{A_3}\, y + B_8 \sinh \sqrt{A_3}\, y + l_4 \cosh \sqrt{\phi_2 + A_5}\, y + l_5 \sinh \sqrt{\phi_2 + A_5}\, y + l_6. \tag{42}
$$

The solutions of the first-order perturbation Eqs. (21), (22), (25) and (26) using the boundary and interface conditions Eqs. (29), (30) can be shown to be

$$
\begin{aligned}
\theta_{11} = \; & B_9 \cos \sqrt{\phi_1 + E^2}\, y + B_{10} \sin \sqrt{\phi_1 + E^2}\, y + r_{14} \cosh 2\sigma y \\
& + r_{15} \sinh 2\sigma y + r_{16} \cosh 2\sqrt{\phi_1 + E^2}\, y + r_{17} \sinh 2\sqrt{\phi_1 + E^2}\, y \\
& + r_{18} \cosh \left(\sigma + \sqrt{\phi_1 + E^2}\right) y + r_{19} \sinh \left(\sigma + \sqrt{\phi_1 + E^2}\right) y \\
& + r_{20} \cosh \left(\sigma - \sqrt{\phi_1 + E^2}\right) y + r_{21} \sinh \left(\sigma - \sqrt{\phi_1 + E^2}\right) y \\
& + r_{22} \cosh \sigma y + r_{23} \sinh \sigma y + r_{24} y \cosh \sqrt{\phi_1 + E^2}\, y \\
& + r_{25} y \sinh \sqrt{\phi_1 + E^2}\, y + r_{26},
\end{aligned} \tag{43}
$$

$$
\begin{aligned}
\theta_{21} = \; & B_{11}\cosh\sqrt{\phi_2+A_5}\,y + B_{12}\sinh\sqrt{\phi_2+A_5}\,y + g_{14}\cosh 2\sqrt{A_3}\,y \\
& + g_{15}\sinh 2\sqrt{A_3}\,y + g_{16}\cosh 2\sqrt{\phi_2+A_5}\,y + g_{17}\sinh 2\sqrt{\phi_2+A_5}\,y \\
& + g_{18}\cosh\left(\sqrt{A_3}+\sqrt{\phi_2+A_5}\right)y + g_{19}\sinh\left(\sqrt{A_3}+\sqrt{\phi_2+A_5}\right)y \\
& + g_{20}\cosh\left(\sqrt{A_3}-\sqrt{\phi_2+A_5}\right)y + g_{21}\sinh\left(\sqrt{A_3}-\sqrt{\phi_2+A_5}\right)y \\
& + g_{22}\cosh\sqrt{A_3}\,y + g_{23}\sinh\sqrt{A_3}\,y + g_{24}y\cosh\sqrt{\phi_2+A_5}\,y \\
& + g_{25}y\sinh\sqrt{\phi_2+A_5}\,y + g_{26},
\end{aligned} \tag{44}
$$

$$
\begin{aligned}
u_{11} = \; & B_{13}\cosh\sigma\,y + B_{14}\sinh\sigma\,y + l_7\cosh\sqrt{\phi_1+E^2}\,y \\
& + l_8\sinh\sqrt{\phi_1+E^2}\,y + l_9\cosh 2\sigma\,y + l_{10}\sinh 2\sigma\,y \\
& + l_{11}\cosh 2\sqrt{\phi_1+E^2}\,y + l_{12}\sinh 2\sqrt{\phi_1+E^2}\,y \\
& + l_{13}\cosh\left(\sigma+\sqrt{\phi_1+E^2}\right)y + l_{14}\sinh\left(\sigma+\sqrt{\phi_1+E^2}\right)y \\
& + l_{15}\cosh\left(\sigma-\sqrt{\phi_1+E^2}\right)y + l_{16}\sinh\left(\sigma-\sqrt{\phi_1+E^2}\right)y \\
& + l_{17}\,y\cosh\sigma\,y + l_{18}\,y\sinh\sigma\,y + l_{19}\,y\cosh\sqrt{\phi_1+E^2}\,y \\
& + l_{20}\,y\sinh\sqrt{\phi_1+E^2}\,y + l_{21},
\end{aligned} \tag{45}
$$

$$
\begin{aligned}
u_{21} = \; & B_{15}\cosh\sqrt{A_3}\,y + B_{16}\sinh\sqrt{A_3}\,y + l_{22}\cosh\sqrt{\phi_2+A_5}\,y \\
& + l_{23}\sinh\sqrt{\phi_2+A_3}\,y + l_{24}\cosh 2\sqrt{A_3}\,y + l_{25}\sinh 2\sqrt{A_3}\,y \\
& + l_{26}\cosh 2\sqrt{\phi_2+A_5}\,y + l_{27}\sinh 2\sqrt{\phi_2+A_5}\,y \\
& + l_{28}\cosh\left(\sqrt{A_3}+\sqrt{\phi_2+A_5}\right)y + l_{29}\sinh\left(\sqrt{A_3}+\sqrt{\phi_2+A_5}\right)y \\
& + l_{30}\cosh\left(\sqrt{A_3}-\sqrt{\phi_2+A_5}\right)y + l_{31}\sinh\left(\sqrt{A_3}-\sqrt{\phi_2+A_5}\right)y \\
& + l_{32}\,y\cosh\sqrt{A_3}\,y + l_{33}\,y\cosh\sqrt{A_3}\,y + l_{34}\,y\cosh\sqrt{\phi_2+A_5}\,y \\
& + l_{35}\,y\sinh\sqrt{\phi_2+A_5}\,y + l_{36}.
\end{aligned} \tag{46}
$$

The expressions for the constants that appear in the above solutions for the heat absorption case are given in the Appendix.

2.3. The Nusselt number. Apart from the velocity and temperature distribution in the channel, it is important to determine the rate of heat transfer between the plates and fluid. The rate of heat transfer through the channel walls to the fluid is given by

$$
q = K\left(\frac{\partial T}{\partial y}\right)_{y=+h_1,-h_2}.
$$

A measure of the effectiveness of heat transfer is provided by the Nusselt number, being proportional to heat transfer rate over channel height divided by temperature difference. This number at the right and left walls is given, respectively, by

$$
\mathrm{Nu}_R = (1+h)\left(\frac{\partial\theta}{\partial y}\right)_{y=-1} \quad \text{and} \quad \mathrm{Nu}_L = (1+h^{-1})\left(\frac{\partial\theta}{\partial y}\right)_{y=-1}.
$$

The variation of the Nusselt numbers at the left and right walls for different physical parameters will be discussed below.

3. Results and Discussion

Eqs. (31) – (46) for the velocity, temperature distributions and heat transfer coefficient are evaluated numerically and the results are discussed in this section. Since the problem involves too many physical parameters we fix some of them, namely, $P = -5.0$, $\mathrm{Re} = 5.0$ (for heat generation case), $\mathrm{Re} = 2.0$ (for heat absorption case), $n = 1.0$, $k = 1.0$, $K = 1.0$, $b = 1.0$, and $\varepsilon = 0.1$ for the sake of conciseness for all numerical computations and analyze the effect of other important nondimensional parameters on flow and heat transfer. In each of the figures, all the other parameters except the varying one are chosen from the set $(\sigma, \mathrm{Gr}, m, h) = (2.0, 5.0, 1.0, 1.0)$. The velocity and temperature distributions are computed up to the first-order approximation based on the analytical solutions and are depicted in Figs. 1 – 18 and in Figs. 19 – 20 based on a finite difference numerical solution. The details of the numerical method and step sizes employed are given in more detail by Chamkha [35]. A measure of the effectiveness of the heat transfer, namely, the Nusselt number is computed for different values of m, Gr, ϕ, h, and E and presented in Tables 1 and 2 for heat absorption and generation conditions, respectively.

The results reported in Figs. 1 – 12 are for the heat absorption case while Figs. 13 – 18 are for the heat generation case. These results illustrate the effects of different physical parameters such as the Grashof number, viscosity ratio, width ratio, porous medium parameter, heat generation or absorption coefficient, and the radiation parameter on the velocity and temperature profiles in the channel.

The effect of Gr on the velocity and temperature profiles is shown in Figs. 1 and 7. Physically speaking, an increase in the value of Gr corresponds to an increase in the buoyancy force and, therefore, buoyancy-induced flow in the channel. This increase in flow due to stronger buoyancy effects causes more convection interaction, producing a higher temperature state. The maximum velocity in the channel is predicted to exist close to the interface for low Gr values, and the temperature filed is nonlinear. As Gr increases, the maximum velocity increases and moves away from the interface toward the wall in region I ($0 \leq y \leq 1$). These behaviors are depicted in the increases of both u and θ as Gr increases, shown in Figs. 1 and 7.

The effects of the viscosity and width ratios (m and h) on the velocity profiles are shown in Figs. 2 and 3 and on the temperature profiles in Figs. 8 and 9, respectively. As expected, the maximum velocity in the channel occurs at the interface ($y = 0$) for $h = 1$ and almost there for $m = 1$. Also, based on the definition of m and h, for $m < 1$ and $h < 1$, the maximum velocity occurs region I ($0 \leq y \leq 1$). However, for $m > 1$ and $h > 1$, the peak velocity occurs in region II ($-1 \leq y \leq 0$) and its location moves toward the wall further and further as m and h are increased further and further. As for the temperature profiles, it is seen that the degree of nonlinearity in the temperature profiles increases as the width ratio h increases. For $h = 0.01$, the value of θ is almost zero in region II while for $h = 3.0$ a relative maximum exists there and a relative minimum is predicted in region I. As obvious from the results, increasing the values of m and/or h has the effect of promoting the flow and enhancing the thermal state in the channel.

The effect of the porous medium parameter σ on the velocity and temperature fields is shown in Figs. 7 and 10, respectively. The presence of a porous medium in the channel has a tendency to produce a flow restriction causing the velocity profile to decrease. This decrease in the flow speed continues, and the velocity profile becomes flatter as σ increases. As a result of this, the temperature

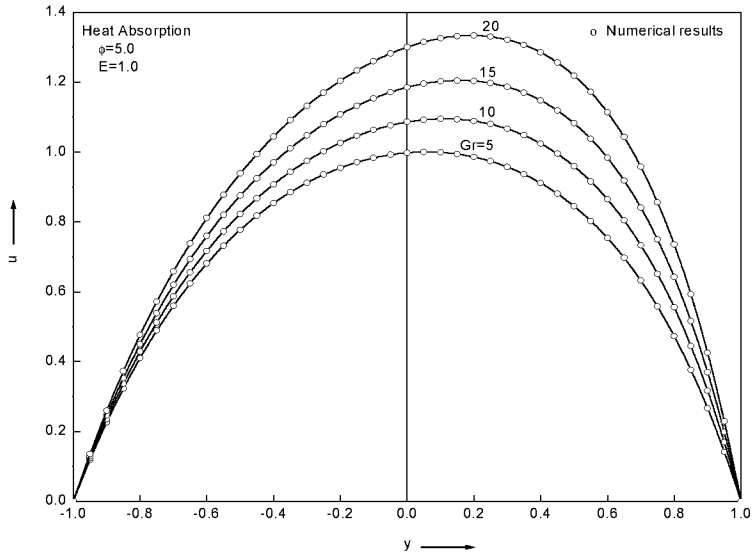

Fig. 1. Velocity profiles for different values of Grashof number Gr.

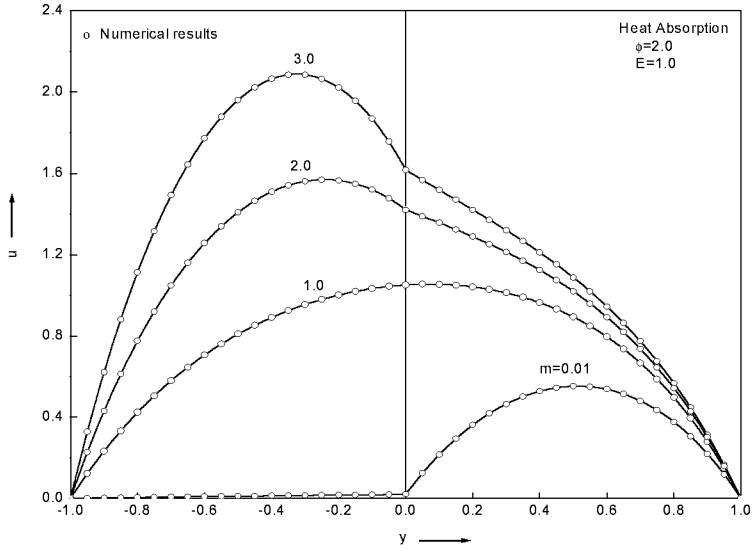

Fig. 2. Velocity profiles for different values of the viscosity ratio m.

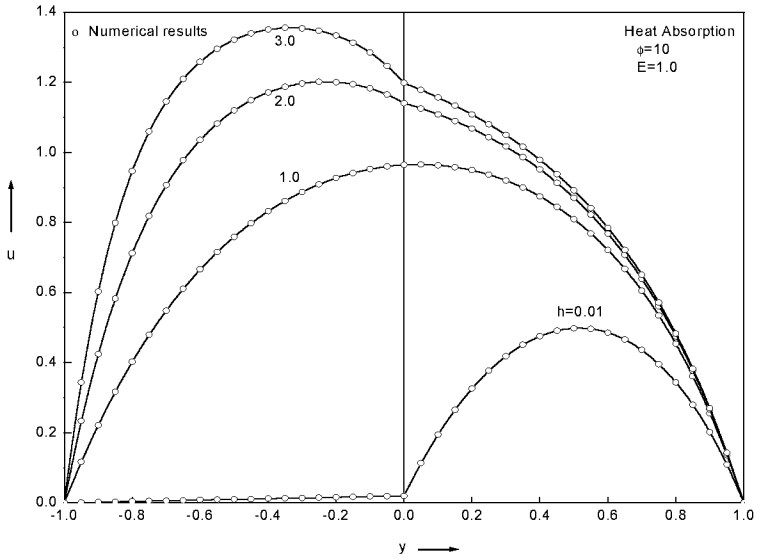

Fig. 3. Velocity profiles for different values of the heights ratio h.

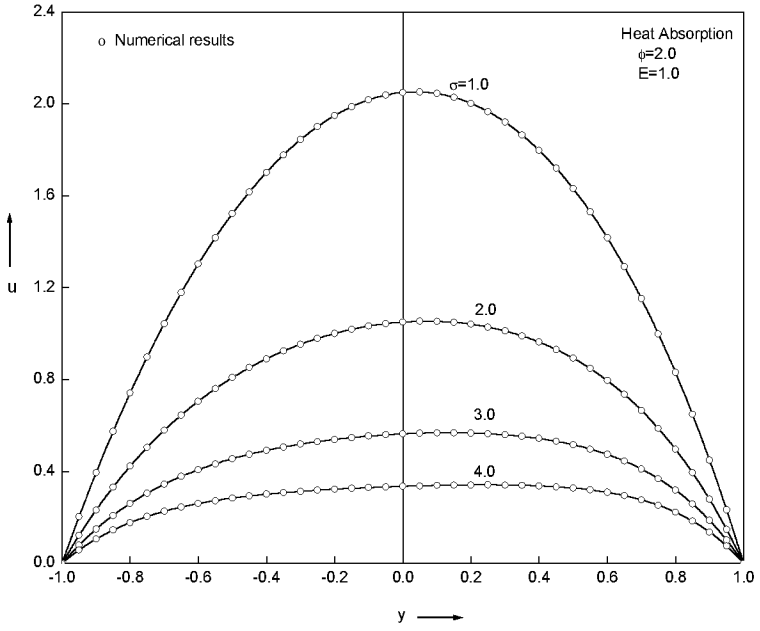

Fig. 4. Velocity profiles for different values of the porous medium parameter σ.

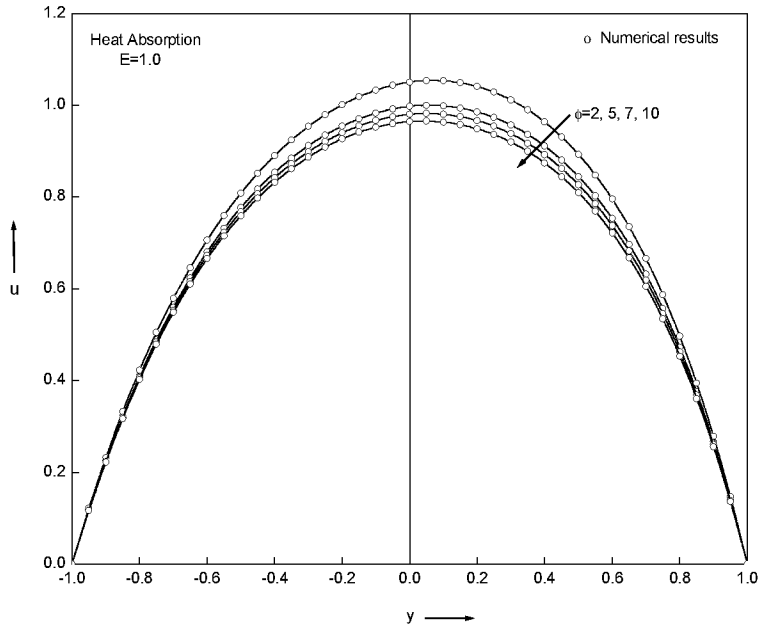

Fig. 5. Velocity profiles for different values of the heat absorption coefficient ϕ.

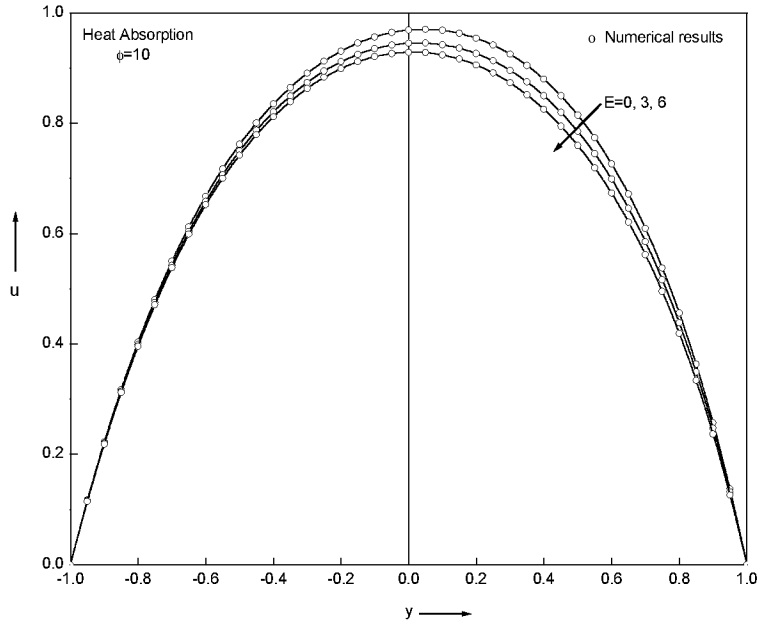

Fig. 6. Velocity profiles for different values of the radiation parameter E.

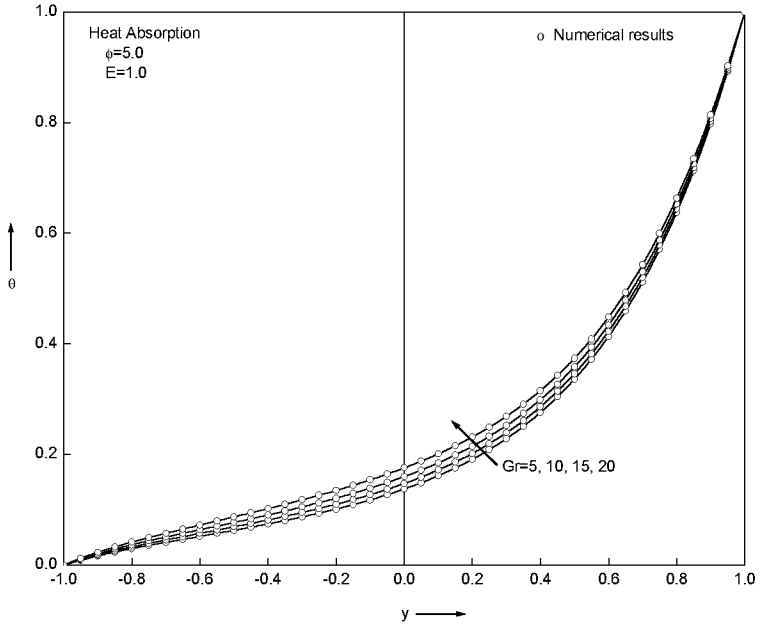

Fig. 7. Temperature profiles for different values of Grashof number Gr.

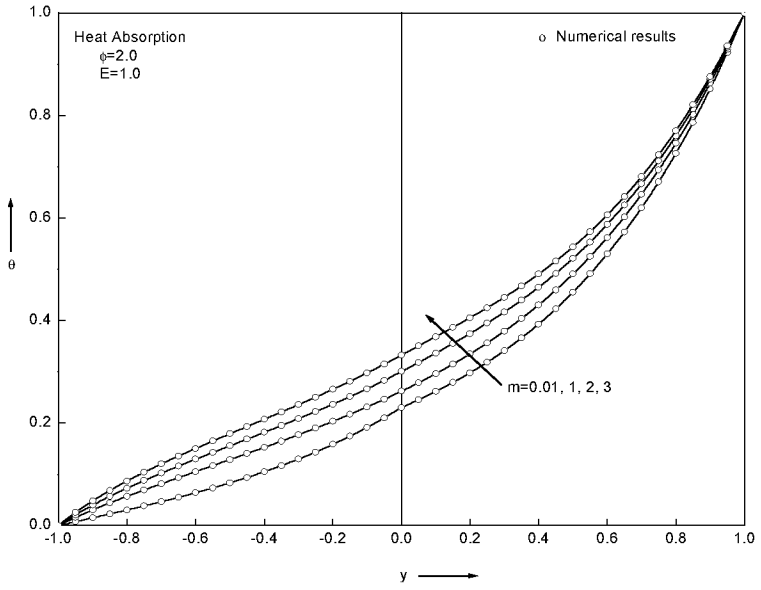

Fig. 8. Temperature profiles for different values of the viscosity ratio m.

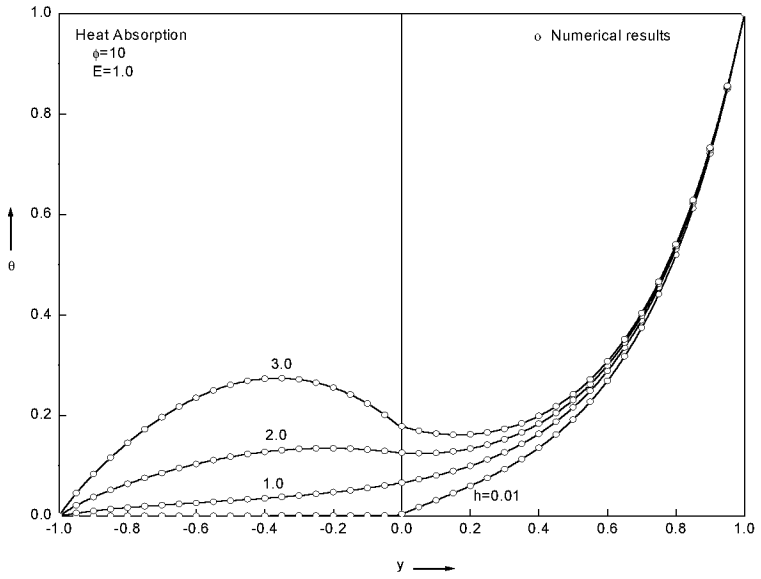

Fig. 9. Temperature profiles for different values of the heights ratio h.

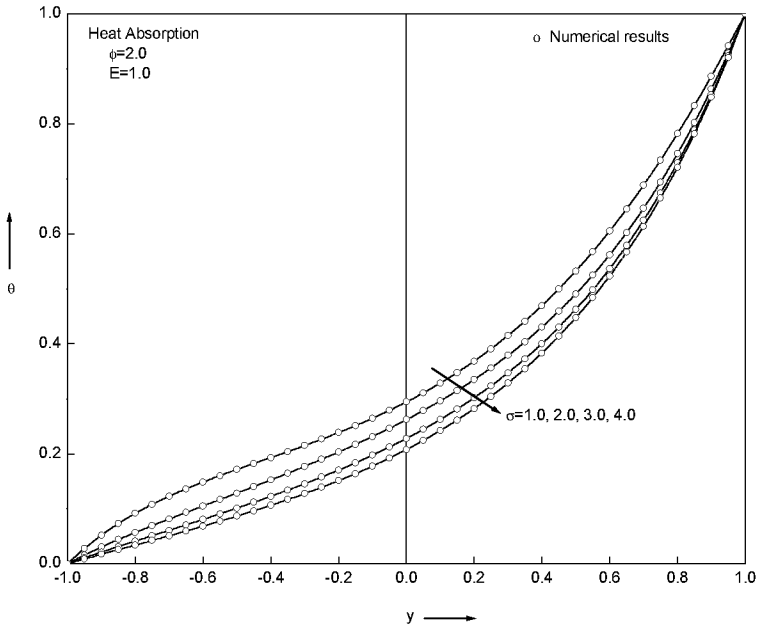

Fig. 10. Temperature profiles for different values of the porous medium parameter σ.

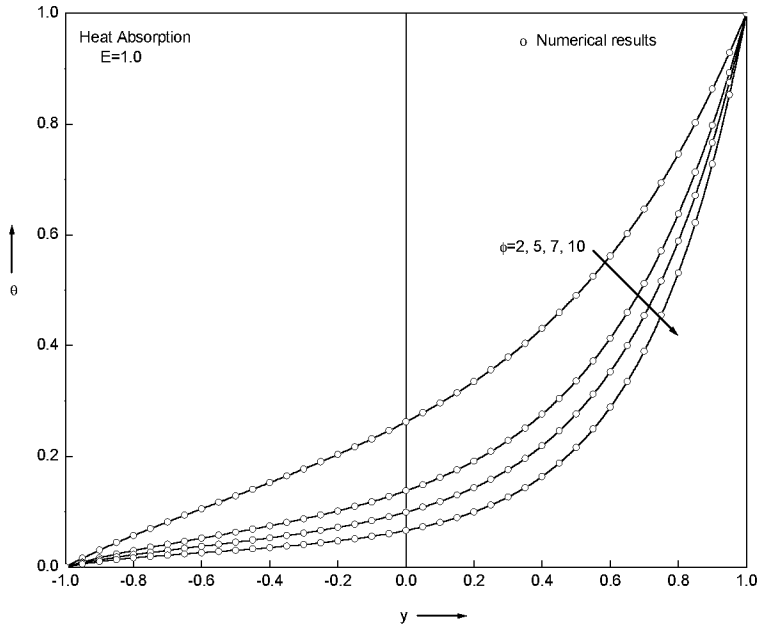

Fig. 11. Temperature profiles for different values of the heat absorption coefficient ϕ.

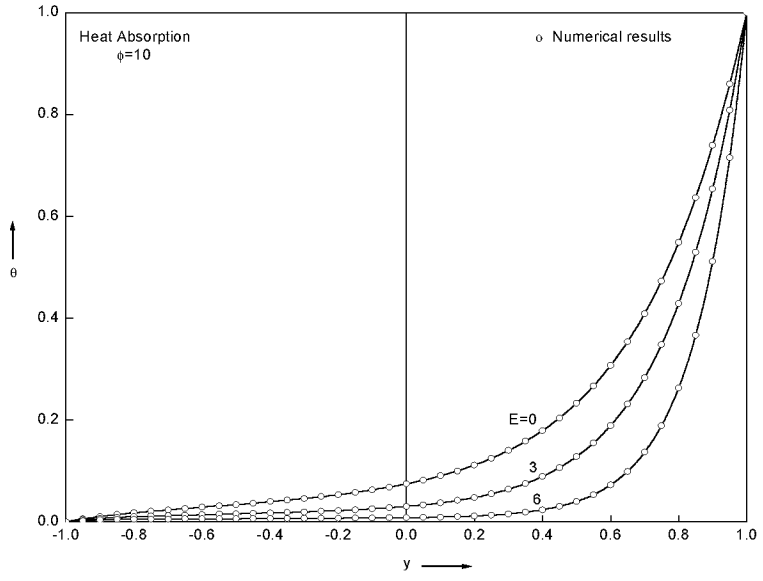

Fig. 12. Temperature profiles for different values of the radiation parameter E.

profile in the channel decreases as σ increases. Therefore, in general, the effect of increasing σ is to suppress the convective motion in the channel.

The effect of the heat absorption coefficient ϕ on the velocity and temperature profiles in the channel is shown in Figs. 5 and 11, respectively. The presence of heat absorption effects of both fluids has the tendency to decrease temperature of both fluids. This causes a decrease in the buoyancy force. This has the direct effect of decreasing the buoyancy-induced flow in the channel. These behaviors are depicted in the decrease in both the velocity and temperature fields as the heat absorption value increases.

Inspection of Eqs. (13) and (15) shows that the radiation effect is very similar to that of heat absorption and the opposite to that of heat generation. Therefore, as expected, the effect of the radiation parameter E is also to decrease the flow velocity and temperature, as seen in Figs. 6 and 12.

The effects of Gr, viscosity ratio, and the porous medium parameter on the velocity and temperature profiles for the case of heat generation are similar to those of the heat absorption case. For this reason, no results for these effects are shown. The effect of the width ratio h on the velocity and temperature fields is shown in Figs. 13 and 16, respectively. A very different behavior is predicted for this case than for the heat absorption case in which the velocity of the fluid in region II ($-1 \leq y \leq 0$) increases while the fluid in region I ($0 \leq y \leq 1$) decreases as h increases. This behavior in the velocity profile as h increases is accompanied with a decrease in the temperature of the fluid in region I and increase in the temperature of the fluid in region II (except for $h = 0.01$ for which $\theta = 0$). For the high value of heat generation coefficient used to obtain Fig. 16 ($\phi = 10$), the dimensionless temperature θ is negative in region II for almost all values of h used, except $h = 0.01$ and partly negative in region I only for $h = 2$ and 3.

The effect of the heat generation coefficient ϕ on the velocity and temperature profiles is shown in Figs. 14 and 17, respectively. The presence of heat generation in both fluids in the channel has the tendency to increase the temperature of these fluids. Therefore, for $\mathrm{Gr} > 0$, the buoyancy effects increase, which results in higher fluid velocities in the channel. For the parametric condition employed to produced these figures, it is predicted that the velocity profile is flat in the middle of the channel for small values of ϕ and a distinctive peak starts to form for higher values of ϕ. The location of the maximum velocity in the channel tends to move toward the wall in region I as ϕ increases. As for the temperature field, the temperatures of both fluids increase as ϕ increases (except for $\phi = 10$ in region II for which the temperature predict a relative minimum below that for $\phi = 4$). Also, the values of θ are all negative in region II and are partly negative in region I except for $\phi = 10$ for which θ is positive there.

The effect of the radiation parameter E counteracts the effect of heat generation [see Eqs. (13) and (15)]. In the absence of thermal radiation and presence of high heat generation effect, a backflow occurs in region I and a distinctive peak in the velocity of the fluid in region II occurs. However, in the presence of thermal radiation with $\phi = 10$, a very different behavior takes place in which both the velocity and temperature of both fluids increase as E increases, as seen in Figs. 15 and 18.

Figs. 19 and 20 present fully numerical results for the velocity and temperature profiles in the channel for various values of the perturbation parameter $\varepsilon = \mathrm{Pr}\,\mathrm{Ec}$ in the presence or absence of heat generation or absorption, respectively. It should be noted that ε represents the effects of viscous and porous medium dissipations [see Eqs. (13) and (15)]. It is obvious from these figures that as the viscous and porous medium dissipations increase, the velocity and temperature fields of the fluids in the channel decrease for the heat generation case and increase for the cases of heat absorption and no source/sink case.

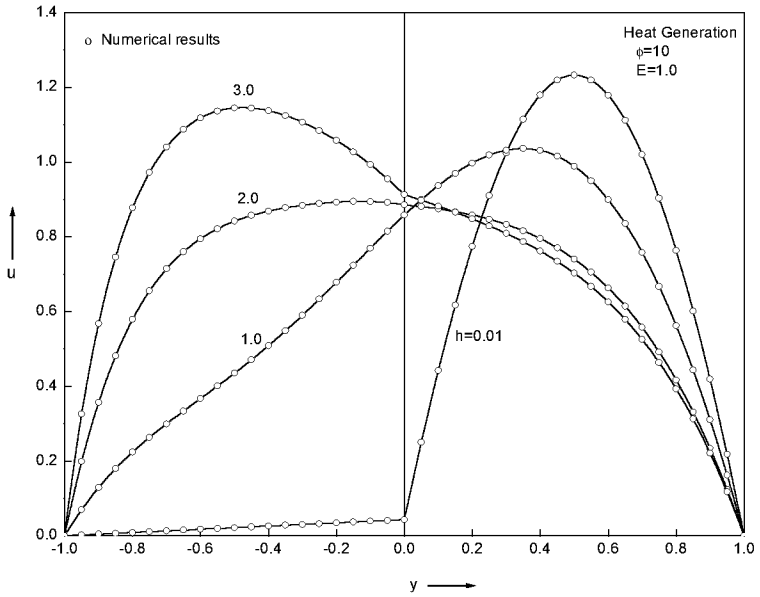

Fig. 13. Velocity profiles for different values of the heights ratio h.

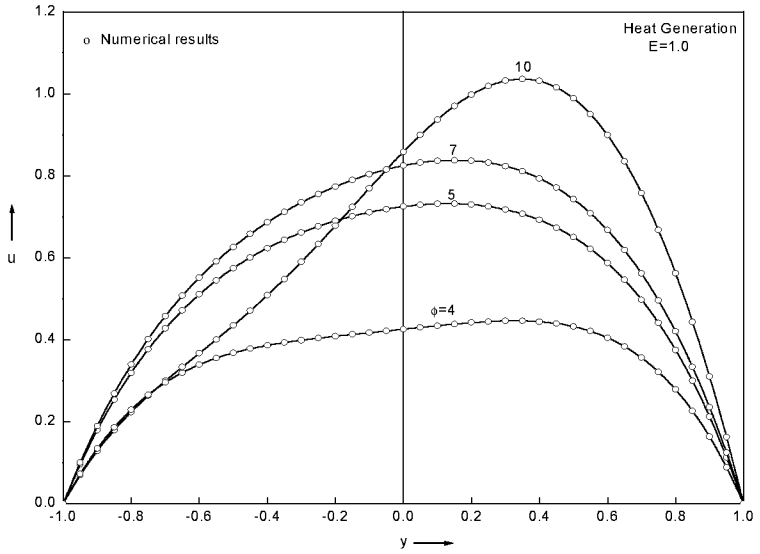

Fig. 14. Velocity profiles for different values of the heat generation coefficient ϕ.

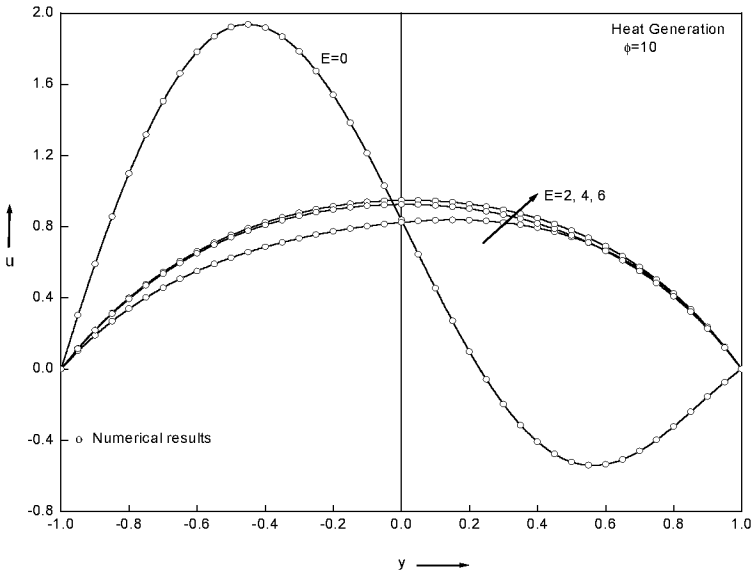

Fig. 15. Velocity profiles for different values of the radiation parameter E.

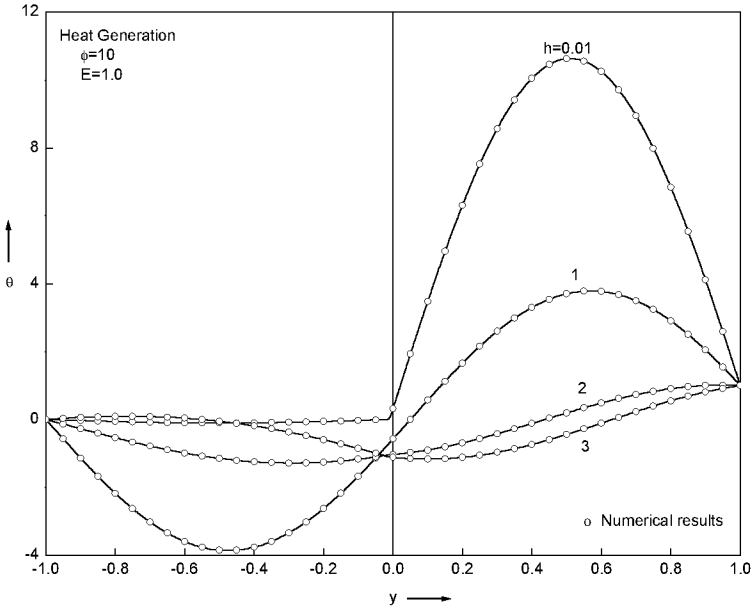

Fig. 16. Temperature profiles for different values of the heights ratio h.

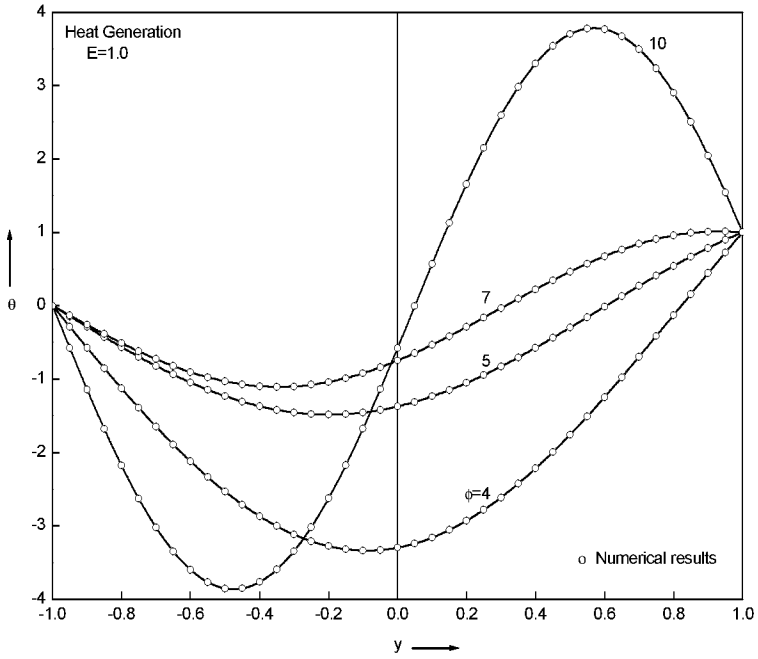

Fig. 17. Temperature profiles for different values of the heat generation coefficient ϕ.

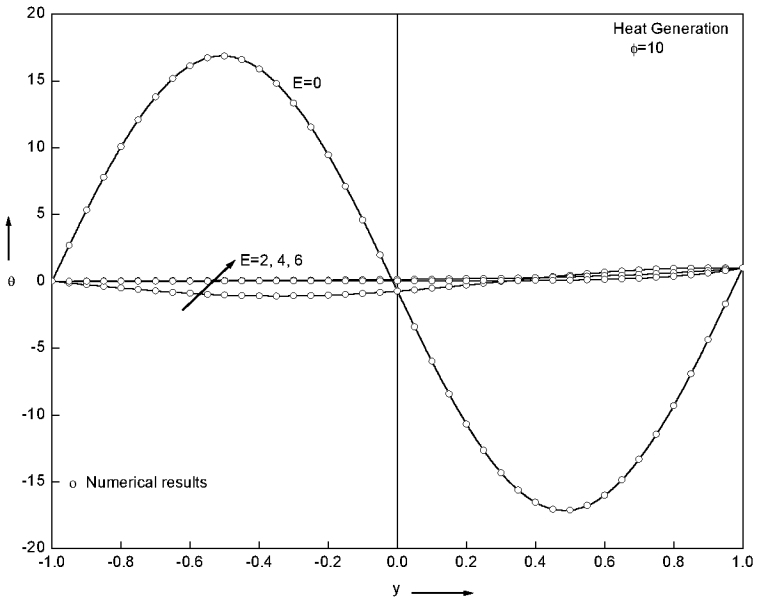

Fig. 18. Temperature profiles for different values of the radiation parameter E.

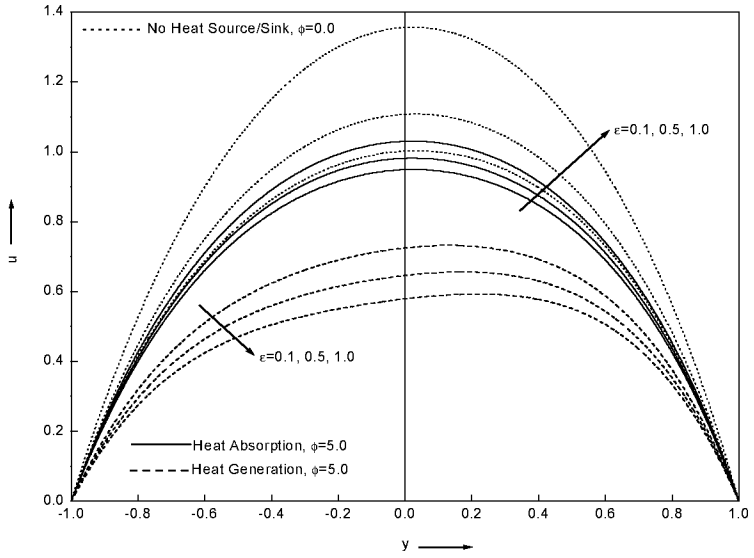

Fig. 19. Velocity profiles for different values of $\varepsilon = \mathrm{Pr}\,\mathrm{Ec}$.

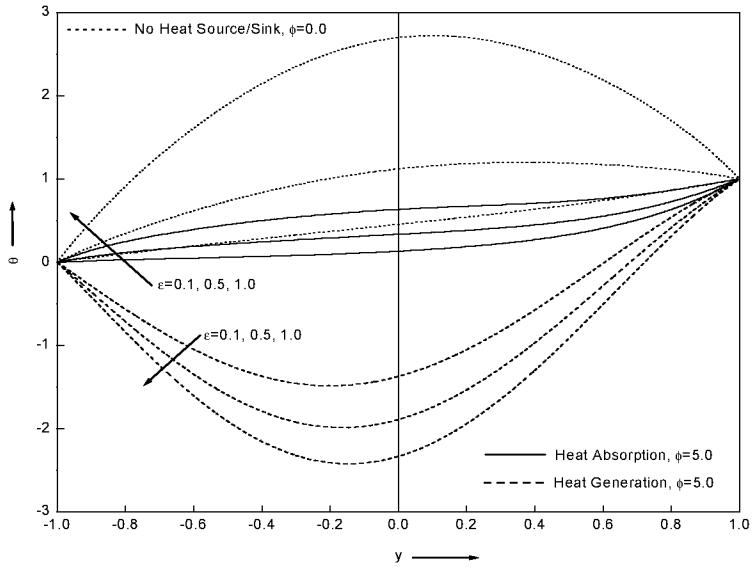

Fig. 20. Temperature profiles for different values of $\varepsilon = \mathrm{Pr}\,\mathrm{Ec}$.

Table 1.
Effects of σ, Gr, ϕ, m, and E on Nu_R and Nu_L for the heat absorption case

σ	Nu_R	Nu_L
1.0	2.336192	1.197124
2.0	2.915716	0.6623973
3.0	3.157914	0.4476993
4.0	3.265619	0.3558058
Gr		
5	4.473281	0.3828449
10	4.357183	0.4208313
15	4.214084	0.4677473
20	4.036236	0.5276141
$\phi_1 = \phi_2 = \phi$		
2.0	2.915716	0.6623973
5.0	4.473281	0.3828449
7.0	5.263293	0.3065221
10.	6.258929	0.2452295
m		
0.01	3.164446	0.2977711
1.0	2.915716	0.6623973
2.0	2.750695	0.8919632
3.0	2.638495	1.097739
E		
0.0	5.946386	0.2613563
3.0	8.330048	0.1791406
6.0	12.98330	0.1205041

Table 2.
Effects of ϕ, h, and E on Nu_R and Nu_L for the heat generation case

ϕ	Nu_R	Nu_L
4.0	10.87593	-11.45363
5.0	3.852451	-5.722180
7.0	-0.8213282	-5.209809
10.	-22.18237	-23.10662
h		
0.01	-32.41842	-32.61535
1.0	-22.18237	-23.10662
2.0	-1.310670	-4.030397
3.0	5.931211	1.085669
E		
0.0	108.2887	108.4366
2.0	-0.8213282	-5.209809
4.0	4.532099	0.3632726
6.0	9.786690	0.1523603

The variations of the Nusselt numbers at the right and left walls of the channel (Nu_R and Nu_L) with different physical parameters are shown in Tables 1 and 2 for the heat absorption and heat generation cases, respectively. It can be observed from Table 1 that for the heat absorption case as Nu_R increases, Nu_L decreases. However, Table 2 shows clearly that this is not the case for the heat generation condition. Also, is seen from Table 1 that increasing either the porous medium parameter, heat absorption coefficient, or the radiation parameter increases the rate of heat transfer at the right wall. However, increasing either Gr or the viscosity ratio decreases the right-wall Nusselt number Nu_R. From Table 2, it is clear that as either the width ratio or the radiation parameter increases, the Nusselt numbers at the right and left walls increase (with a couple of exceptions, for $E = 0$ and 6). On the other hand, as the heat generation coefficient increases, Nu_R decreases while Nu_L increases (with the exception of $\phi = 10$).

Conclusion

The problem of steady mixed convection flow of two immiscible fluids in a vertical porous stratum in the presence of a heat source or sink and thermal radiation effects was investigated analytically and numerically. Both fluids were assumed to be in thermal equilibrium with the porous medium. Separate closed-form solutions for each fluid were obtained, taking into consideration suitable interface matching conditions. The closed-form results were numerically evaluated and graphically presented for various parameters for heat absorption and generation conditions. It was found that the flow and heat transfer characteristics can be effectively controlled by the properties of the two fluids as well as the thermal radiation parameter, heat generation or absorption coefficient, and porous medium parameter.

REFERENCES

1. Combarnous, M. A. and Bories, S. A, Hydrothermal Convection in Saturated Porous Media, *Adv. Hydrosci.*, 1975, **10**, pp. 231–307.
2. Cheng, P., Heat Transfer in Geothermal Systems, *Adv. Heat Transfer*, 1978, **14**, pp. 1–105.
3. Rudraiah, N., Non-Linear Convection in a Porous Medium with Convective Acceleration and Viscous Force, *Arab. J. Sci. Eng.*, 1984, **9**, pp. 153–167.
4. Rudraiah, N., Heat and Mass Transfer in Composite Materials (Presidential Address), In: *Section of Mathematics, Indian Science Congress*, 1988.
5. Nield, D. A., Recent Research on Convection in a Porous Medium, In: *Proc. CSIRO / DSIR Seminar on Convective Flows in Porous Media*, Wellington, New Zealand, 1984, pp. 717–722.
6. Kaviany, M., *Principles of Heat Transfer in Porous Media*, Springer-Verlag, New York, 1991.
7. Nield, D. A. and Bejan, A., *Convection in Porous Media*, Springer-Verlag, New York, 1992.
8. Prasad, V., Kulacki, F., and Keyhani, M., Natural Convection in Porous Media, *J. Fluid. Mech.*, 1985, **150**, pp. 89–119.
9. Vafai, K. and Tien, C. L., Boundary and Inertia Effects on Flow and Heat Transfer in a Porous Medium, *Int. J. Heat Mass Transfer*, 1981, **24**, pp. 195–203.
10. Vafai, K. and Tien, C. L., Boundary and Inertial Effects on Convective Mass Transfer in Porous Media, *Int. J. Heat Mass Transfer*, 1982, **25**, pp. 1183–1190.
11. Beckermann, C., Viskanta, R., and Ramadhyani, A., Numerical study of a Non-Darcian Natural Convection in a Vertical Enclosure Filled with a Porous Medium, *Numer. Heat Transfer*, 1986, **10**, pp. 557–570.

12. Georgiadis, J. and Catton, I., Prandtl Number Effect on Benard Convection in Porous Media, *ASME J. Heat Transfer*, 1986, **10**, pp. 284–290.
13. Lauriat, G. and Prasad, V., Natural Convection in a Vertical Porous Cavity: A Numerical Study for Brinkman-Extended Darcy Formulation, In: *Natural Convection in a Porous Media*, ASME, New York, 1986, pp. 13–22.
14. Prasad, V., Convection Flow Interaction and Heat Transfer Between Fluid and Porous Layers, In:*Proc. NATO Adv. Study Inst. Convective Heat and Mass Transfer in Porous Media*, 1990, Turkey.
15. Malashetty, M. S., Umavathi, J. C., and Prathapkumar, J., Convective Flow and Heat Transfer in an Inclined Composite Porous Medium, *J. Por. Media*, 2001, **14**, pp. 15–22.
16. Bejan, A., *Heat Transfer*, Wiley, New York, 1993.
17. Grief, R., Habib, I. S., and Lin, J. C., Laminar Convection of a Radiating Gas in a Vertical Channel, *J. Fluid Mech.*, 1971, **46**, pp. 513–520.
18. Gupta, P. S. and Gupta, A. S., Radiation Effect on Hydromagnetic Convection in a Vertical Channel, *Int. J. Heat Mass Transfer*, 1974, **17**, pp. 1439–1447.
19. Viskanta, R. and Grosh, R. J., Heat Transfer by Simultaneous Conduction and Radiation in an Arbitrary Medium, *J. Heat Transfer*, 1962, **84**, pp. 63–72.
20. Cess, R. D., Mighdoll, P., and Tiwari, S. N., Infrared Radiative Heat Transfer in Nongray Gases, *Int. J. Heat Mass Transfer*, 1967, **10**, pp. 1521–1532.
21. Cogley, A. C., Vincenti, W. G., and Gilles, S. E., Differential Approximation for Radiative Transfer in a Non-Gray Gas Near Equilibrium, *AIAA J.*, 1968, **6**, pp. 551–553.
22. Chamkha, A. J., Effects of Heat Absorption and Thermal Radiation on Heat Transfer in a Fluid-Particle Flow Past Surface in the Presence of a Gravity Field, *Int. J. Therm. Sci.*, 1986, **39**, pp. 605–615.
23. Caltagirone, J. P., Convection in a Porous Medium, In: *Convective Transport and Instability Phenomena*, Karlsruhe, Germany, 1982, pp. 199–232.
24. Bear, J., *Dynamics of Fluids in Porous Media*, Elsevier, New York, 1972.
25. Elder, J. W., Steady Free Convection in a Porous Medium Heated from Below, *J. Fluid Mech.*, 1967, **27**, pp. 29–48.
26. Elder, J. W., Transient Convection in a Porous Medium, *J. Fluid Mech.*, 1979, **27**, pp. 609–623.
27. Yih, C. S., *Dynamics of Nonhomogeneous Fluids*, Macmillan, New York, 1965, pp. 197.
28. Raats, P. A. C., The Role of Inertia on the Hydrodynamics of Porous Media, *Arch. Rat. Mech. Anal.*, 1972, **44**, pp. 267–280.
29. Yamamoto, K. and Yoshida, Z., Flow Through a Porous Wall with Convective Acceleration, *J. Phys. Soc. Japan*, 1974, **37**, pp. 774–779.
30. Tam, C. K. W., The Drag on a Closed Spherical Particles System in Low Reynolds Number Flow, *J. Fluid Mech.*, 1969, **38**, pp. 537–546.
31. Slattery, J. C., Single Phase Flow Through Porous Media, *AIChE J.*, 1969, **15**, pp. 866–872.
32. Williams, W. O., Constitutive Equations for Flow of an Incompressible Viscous Fluid Through a Porous Medium, *Quart. J. Appl. Math.*, 1978, **36**, pp. 255–267.
33. Rudraiah, N., Chandarasekhara, B. C., Veerabhadraiah, R., and Nagaraj, S. T., *Some Flow Problems in Porous Media*, Post-Graduate Studies Appl. Math., Bangalore, 1979.
34. Yamamoto, K. and Imamura, N., Flow with Convective Acceleration Through a Porous Medium, *J. Eng. Math.*, 1976, **10**, pp. 41–54.
35. Chamkha, A. J., Flow of Two-Immiscible Fluids in Porous and Non-Porous Channels, *ASME J. Fluids Eng.*, 2000, **122**, pp. 117–124.

Appendix

Heat absorption case.

$$A_1 = \frac{\mathrm{Gr}}{\mathrm{Re}}; \qquad A_2 = \frac{\mathrm{Gr}\, bmnh^2}{\mathrm{Re}}; \qquad A_3 = \sigma h^2 k;$$

$$A_4 = mh^2 P; \qquad A_5 = E^2 h^2 K; \qquad A_6 = \frac{K}{m}; \qquad A_7 = K\sigma^2 h^2 \frac{K}{m};$$

$$B_1 = \frac{1 - B_2 \sinh\sqrt{\phi_1 + E^2}}{\cosh\sqrt{\phi_1 + E^2}}; \quad B_3 = \frac{1 - B_2 \sinh\sqrt{\phi_1 + E^2}}{\cosh\sqrt{\phi_1 + E^2}}; \quad B_4 = \frac{B_3 \cosh\sqrt{\phi_2 + A_5}}{\sinh\sqrt{\phi_2 + A_5}};$$

$$B_2 = \frac{\sqrt{\phi_2 + A_5}\cosh\sqrt{\phi_2 + A_5}}{\sqrt{\phi_2 + A_5}\sinh\sqrt{\phi_1 + E^2}\cosh\sqrt{\phi_2 + A_5} + Kh\sqrt{\phi_1 + E^2}\cosh\sqrt{\phi_1 + E^2}\sinh\sqrt{\phi_2 + A_5}};$$

$$B_5 = \frac{G_1 - B_6 \sinh\sigma}{\cosh\sigma}; \quad B_6 = \frac{D_1 \cosh\sqrt{A_3} - D_6 \cosh\sigma}{\sinh\sigma\cosh\sqrt{A_3} + D_5 \sinh\sqrt{A_3}\cosh\sigma}; \quad B_7 = B_5 - D_2;$$

$$B_8 = \frac{B_7 \cosh\sqrt{A_3} - D_3}{\sinh\sqrt{A_3}}; \qquad B_9 = \frac{D_7 - B_{10}\sinh\sqrt{\phi_1 + E^2}}{\cosh\sqrt{\phi_1 + E^2}};$$

$$B_{10} = \frac{\sqrt{\phi_2 + A_5} D_7 \cosh\sqrt{\phi_2 + A_5} - D_{11}\sqrt{\phi_2 + A_5}\cosh\sqrt{\phi_1 + E^2}}{\sqrt{\phi_2 + A_5}\sinh\sqrt{\phi_1 + E^2}\cosh\sqrt{\phi_2 + A_5} + Kh\sqrt{\phi_1 + E^2}\cosh\sqrt{\phi_1 + E^2}\sinh\sqrt{\phi_2 + A_5}};$$

$$B_{11} = B_9 - D_8; \qquad B_{12} = \frac{B_{11}\cosh\sqrt{\phi_2 + A_5} - D_9}{\sinh\sqrt{\phi_2 + A_5}}; \qquad B_{13} = \frac{D_{12} - B_{14}\sinh\sigma}{\cosh\sigma};$$

$$B_{14} = \frac{\sqrt{A_3} D_{12}\cosh\sqrt{A_3} - \sqrt{A_3} D_{16}\cosh\sigma}{\sqrt{A_3}\sinh\sigma\cosh\sqrt{A_3} + mh\sigma\cosh\sigma\sinh\sqrt{A_3}};$$

$$B_{15} = B_{13} - D_{13}; \qquad B_{16} = \frac{B_{15}\cosh\sqrt{A_3} - D_{14}}{\sinh\sqrt{A_3}};$$

$$D_1 = -l_3 - l_1\cosh\sqrt{\phi_1 + E^2} - l_2\sinh\sqrt{\phi_1 + E^2}; \qquad D_2 = l_4 + l_6 - l_1 - l_3;$$

$$D_3 = -l_4\cosh\sqrt{\phi_2 + A_5} + l_5\sinh\sqrt{\phi_2 + A_5} - l_6; D_4 = l_5\sqrt{\phi_2 + A_5} - mhl_2\sqrt{\phi_1 + E^2};$$

$$D_5 = \frac{mh\sigma}{\sqrt{A_3}}; \qquad D_6 = \frac{D_3\sqrt{A_3} - D_4\sinh\sqrt{A_3} + D_2\sqrt{A_3}\cosh\sqrt{A_3}}{\sqrt{A_3}};$$

$$D_7 = -r_{14}\cosh 2\sigma + r_{15}\sinh 2\sigma - r_{16}\cosh 2\sqrt{\phi_1 + E^2} + r_{17}\sinh 2\sqrt{\phi_1 + E^2}$$
$$-r_{18}\cosh\left(\sigma + \sqrt{\phi_1 + E^2}\right) - r_{19}\sinh\left(\sigma + \sqrt{\phi_1 + E^2}\right)$$
$$-r_{20}\cosh\left(\sigma - \sqrt{\phi_1 + E^2}\right) - r_{21}\sinh\left(\sigma - \sqrt{\phi_1 + E^2}\right)$$
$$-r_{22}\cosh\sigma - r_{23}\sinh\sigma - r_{24}\cosh\sqrt{\phi_1 + E^2} - r_{25}\sinh\sqrt{\phi_1 + E^2} + r_{26};$$

$$D_8 = g_{14} + g_{16} + g_{18} + g_{20} + g_{22} + g_{26} - r_{14} - r_{16} - r_{18} - r_{19} - r_{22} - r_{26};$$

$$D_9 = -g_{14}\cosh 2\sqrt{A_3} + g_{15}\sinh 2\sqrt{A_3} - g_{16}\cosh 2\sqrt{\phi_2 + A_5} + g_{17}\sinh\sqrt{\phi_2 + A_5}$$
$$-g_{18}\cosh\left(\sqrt{A_3} + \sqrt{\phi_2 + A_5}\right) + g_{19}\sinh\left(\sqrt{A_3} + \sqrt{\phi_2 + A_5}\right)$$
$$-g_{20}\cosh\left(\sqrt{A_3} - \sqrt{\phi_2 + A_3}\right) + g_{21}\sinh\left(\sqrt{A_3} - \sqrt{\phi_2 + A_5}\right) - g_{22}\cosh\sqrt{A_3}$$
$$+g_{23}\sinh\sqrt{A_3} + g_{24}\cosh\sqrt{\phi_2 + A_5} - g_{25}\sinh\sqrt{\phi_2 + A_5} - g_{26};$$

$$D_{10} = -g_{15}2\sqrt{A_3} - g_{17}2\sqrt{\phi_2 + A_5} - g_{20}\left(\sqrt{A_3} + \sqrt{\phi_2 + A_5}\right)$$
$$-g_{21}\left(\sqrt{A_3} - \sqrt{\phi_2 + A_5}\right) - g_{23}\sqrt{A_3} - g_{24} + 2Kh\sigma r_{15} + 2Kh\sqrt{\phi_1 + E^2}\, r_{17}$$
$$+r_{19}Kh\left(\sigma + \sqrt{\phi_1 + E^2}\right) + r_{21}Kh\left(\sigma - \sqrt{\phi_1 + E^2}\right) + r_{23}Kh\sigma + Khr_{24};$$

$$D_{11} = \frac{D_9\sqrt{\phi_2 + A_5} + D_8\sqrt{\phi_2 + A_5}\cosh\sqrt{\phi_2 + A_5} - D_{10}\sinh\sqrt{\phi_2 + A_5}}{\sqrt{\phi_2 + A_5}};$$

$$D_{12} = -l_7\cosh\sqrt{\phi_1 + E^2} - l_8\sinh\sqrt{\phi_1 + E^2} - l_9\cosh 2\sigma - l_{10}\sinh 2\sigma$$
$$-l_{11}\cosh 2\sqrt{\phi_1 + E^2} - l_{12}\sinh 2\sqrt{\phi_1 + E^2} - l_{13}\cosh\left(\sigma + \sqrt{\phi_1 + E^2}\right)$$
$$-l_{14}\sinh\left(\sigma + \sqrt{\phi_1 + E^2}\right) - l_{15}\cosh\left(\sigma - \sqrt{\phi_1 + E^2}\right) - l_{16}\sinh\left(\sigma - \sqrt{\phi_1 + E^2}\right)$$
$$-l_{17}\cosh\sigma - l_{18}\sinh\sigma - l_{19}\cosh\sqrt{\phi_1 + E^2} - l_{20}\sinh\sqrt{\phi_1 + E^2} - l_{21};$$

$$D_{13} = l_{22} + l_{24} + l_{26} + l_{28} + l_{30} + l_{36} - l_7 - l_9 - l_{11} - l_{13} - l_{14} - l_{21};$$

$$D_{14} = -l_{22}\cosh\sqrt{\phi_2+A_5} + l_{23}\sinh\sqrt{\phi_2+A_5} - l_{24}\cosh 2\sqrt{A_3} + l_{25}\sinh 2\sqrt{A_3}$$
$$-l_{26}\cosh 2\sqrt{\phi_2+A_5} + l_{27}\sinh 2\sqrt{\phi_2+A_5} - l_{28}\cosh\left(\sqrt{A_3}+\sqrt{\phi_2+A_5}\right)$$
$$+l_{29}\sinh\left(\sqrt{A_3}+\sqrt{\phi_2+A_5}\right) - l_{30}\cosh\left(\sqrt{A_3}-\sqrt{\phi_2+A_5}\right) + l_{31}\sinh\left(\sqrt{A_3}-\sqrt{\phi_2+A_5}\right)$$
$$+l_{32}\cosh\sqrt{A_3} - l_{33}\sinh\sqrt{A_3} + l_{34}\cosh\sqrt{\phi_2+A_5} - l_{35}\sinh\sqrt{\phi_2+A_5} - l_{36};$$

$$D_{15} = \sqrt{\phi_2+A_5}\,l_{23} + l_{25} + l_{33} + 2\sqrt{A_3}\,l_{25} + 2\sqrt{\phi_2+A_5}\,l_{25} + 2\sqrt{\phi_2+A_5}\,l_{27}$$
$$+\left(\sqrt{A_3}+\sqrt{\phi_2+A_5}\right)l_{30} + \left(\sqrt{A_3}-\sqrt{\phi_2+A_5}\right)l_{31} - mh\sqrt{\phi_1+E^2}\,l_8 - 2mh\sigma l_{10}$$
$$-2mh\sqrt{\phi_1+E^2}\,l_{12} - mh\left(\sigma+\sqrt{\phi_1+E^2}\right)l_{15} - mh\left(\sigma-\sqrt{\phi_1+E^2}\right)l_{16} - mhl_{18} - mhl_{20}\,;$$

$$D_{16} = \frac{\sqrt{A_3}D_{14} - D_{15}\sinh\sqrt{A_3} + \sqrt{A_3}D_{13}\cosh\sqrt{A_3}}{\sqrt{A_3}}\,;$$

$$g_1 = \frac{A_6A_3B_7^2 + A_7B_8^2 + A_6A_3B_8^2 + A_7B_7^2}{2}\,;$$

$$g_2 = A_6A_3B_7B_8 + A_7B_7B_8;$$

$$g_3 = \frac{A_6l_4^2(\phi_2+A_5) + A_7l_5^2 + A_6l_5^2(\phi_2+A_5) + A_7l_4^2}{2}\,;$$

$$g_4 = A_6l_4l_5(\phi_2+A_5) + A_7l_4l_5;$$

$$g_5 = A_6B_7l_4\sqrt{A_3}\sqrt{\phi_2+A_5} + A_7B_8l_5 + A_6B_8l_5\sqrt{A_3}\sqrt{\phi_2+A_5} + A_7B_7l_4;$$

$$g_6 = A_6B_8l_5\sqrt{A_3}\sqrt{\phi_2+A_5} + A_7B_7l_4 - A_6B_7l_4\sqrt{A_3}\sqrt{\phi_2+A_5} - A_7B_8l_5;$$

$$g_7 = A_6B_7l_5\sqrt{A_3}\sqrt{\phi_2+A_5} + A_7B_8l_4 + A_6B_8l_4\sqrt{A_3}\sqrt{\phi_2+A_5} + A_7B_7l_5;$$

$$g_8 = A_6B_7l_5\sqrt{A_3}\sqrt{\phi_2+A_5} + A_7B_8l_4 - A_6B_8l_4\sqrt{A_3}\sqrt{\phi_2+A_5} - A_7B_7l_5;$$

$$g_9 = 2A_7B_7l_6; \qquad g_{10} = 2A_7B_8l_6; \qquad g_{11} = 2A_7l_4l_6; \qquad g_{12} = 2A_7l_5l_6;$$

$$g_{13} = A_7l_6^2 + \frac{1}{2}A_6A_3B_8^2 + \frac{1}{2}A_7B_7^2 - \frac{1}{2}A_6A_3B_7^2 - \frac{1}{2}A_7B_8^2 + \frac{1}{2}A_6l_5^2(\phi_2+A_5)$$
$$+\frac{1}{2}A_7l_4^2 - \frac{1}{2}A_6l_4^2(\phi_2+A_5) - \frac{1}{2}A_7l_5^2\,;$$

$$g_{14}=\frac{-g_1}{4A_3-(\phi_2+A_5)};\quad g_{15}=\frac{-g_2}{4A_3-(\phi_2+A_5)};\quad g_{16}=\frac{-g_3}{3(\phi_2+A_5)};$$

$$g_{17}=\frac{-g_4}{3(\phi_2+A_5)};\quad g_{18}=\frac{-g_5}{A_3+2\sqrt{A_3}\sqrt{\phi_2+A_5}};\quad g_{19}=\frac{-g_7}{A_3+2\sqrt{A_3}\sqrt{\phi_2+A_5}};$$

$$g_{20}=\frac{-g_6}{A_3-2\sqrt{A_3}\sqrt{\phi_2+A_5}};\quad g_{21}=\frac{-g_8}{A_3-2\sqrt{A_3}\sqrt{\phi_2+A_5}};\quad g_{22}=\frac{-g_9}{A_3-(\phi_2+A_5)};$$

$$g_{23}=\frac{-g_{10}}{A_3-(\phi_2+A_5)};\quad g_{24}=\frac{-g_{12}}{2\sqrt{\phi_2+A_5}};\quad g_{25}=\frac{-g_{11}}{2\sqrt{\phi_2+A_5}};\quad g_{26}=\frac{g_{13}}{\phi_2+A_5};$$

$$l_1=\frac{-A_1B_1}{(\phi_1+E^2)-\sigma^2};\qquad l_2=\frac{-A_1B_2}{(\phi_1+E^2)-\sigma^2};$$

$$l_4=\frac{-A_2B_3}{(\phi_2+A_5)-A_3};\qquad l_5=\frac{-A_2B_4}{(\phi_2+A_5)-A_3};$$

$$l_3=\frac{-P}{\sigma^2};\qquad l_7=\frac{2A_1r_{25}\sqrt{\phi_1+E^2}-A_1B_9(\phi_1+E^2-\sigma^2)}{\left[(\phi_1+E^2)-\sigma^2\right]^2};$$

$$l_6=\frac{-A_4}{A_3};\qquad l_8=\frac{2A_1r_{24}\sqrt{\phi_1+E^2}-A_1B_{10}(\phi_1+E^2-\sigma^2)}{(\phi_1+E^2)-\sigma^2};$$

$$l_9=\frac{-A_1r_{14}}{3\sigma^2};\quad l_{11}=\frac{-A_1r_{16}}{4(\phi_1+E^2)-\sigma^2};\quad l_{12}=\frac{-A_1r_{17}}{4(\phi_1+E^2)-\sigma^2};$$

$$l_{10}=\frac{-A_1r_{15}}{3\sigma^2};\quad l_{13}=\frac{-A_1r_{18}}{(\phi_1+E^2)+2\sigma\sqrt{\phi_1+E^2}};\quad l_{14}=\frac{-A_1r_{19}}{(\phi_1+E^2)+2\sigma\sqrt{\phi_1+E^2}};$$

$$l_{15}=\frac{-A_1r_{20}}{(\phi_1+E^2)-2\sigma\sqrt{\phi_1+E^2}};\quad l_{16}=\frac{-A_1r_{21}}{(\phi_1+E^2)-2\sigma\sqrt{\phi_1+E^2}};\quad l_{17}=\frac{-A_1r_{23}}{2\sigma};$$

$$l_{18}=\frac{-A_1r_{22}}{2\sigma};\quad l_{19}=\frac{-A_1r_{24}}{(\phi_1+E^2)-\sigma^2};\quad l_{20}=\frac{-A_1r_{25}}{-(\phi_1+E^2)-\sigma^2};\quad l_{21}=\frac{A_1r_{26}}{3\sigma^2};$$

$$l_{22}=\frac{2A_7g_{25}\sqrt{\phi_2+A_5}-A_2B_{12}(\phi_2+A_5-A_3)}{(\phi_2+A_5-A_3)^2};\qquad l_{26}=\frac{-A_2g_{16}}{4(\phi_2+A_5)-A_3};$$

$$l_{23}=\frac{2A_2g_{24}\sqrt{\phi_2+A_5}-A_2B_{12}(\phi_2+A_5-A_3)}{(\phi_2+A_5-A_3)^2};\qquad l_{27}=\frac{-A_2g_{17}}{4(\phi_2+A_5)-A_3};$$

$$l_{24}=\frac{-A_2g_{14}}{3A_3};\quad l_{28}=\frac{-A_2g_{18}}{(\phi_2+A_5)+2\sqrt{A_3}\sqrt{\phi_2+A_5}};\quad l_{29}=\frac{-A_2g_{19}}{(\phi_2+A_5)+2\sqrt{A_3}\sqrt{\phi_2+A_5}};$$

$$l_{25}=\frac{-A_2g_{15}}{3A_3};\quad l_{30}=\frac{-A_2g_{20}}{(\phi_2+A_5)-2\sqrt{A_3}\sqrt{\phi_2+A_5}};\quad l_{31}=\frac{-A_2g_{21}}{(\phi_2+A_5)-2\sqrt{A_3}\sqrt{\phi_2+A_5}};$$

$$l_{32}=\frac{-A_2g_{23}}{2\sqrt{A_3}};\quad l_{33}=\frac{-A_2g_{22}}{2\sqrt{A_3}};\quad l_{34}=\frac{-A_2g_{24}}{(\phi_2+A_5)-A_3};$$

$$l_{35}=\frac{-A_2g_{25}}{(\phi_2+A_5)-A_3};\quad l_{36}=\frac{A_2g_{26}}{A_3};$$

$$r_1 = \sigma^2(B_5^2 + B_6^2); \qquad r_2 = 2\sigma^2 B_5^2 B_6^2; \qquad r_4 = l_1 l_2(\phi_1 + E^2) + \sigma^2 l_1 l_2;$$

$$r_3 = \frac{l_1^2(\phi_1 + E^2) + \sigma^2 l_2^2 + l_2^2(\phi_1 + E^2) + \sigma^2 l_1^2}{2};$$

$$r_5 = B_5\sigma l_1\sqrt{\phi_1 + E^2} + \sigma^2 B_6 l_2 + B_6\sigma l_2\sqrt{\phi_1 + E^2} + \sigma^2 B_5 l_1;$$

$$r_6 = B_6\sigma l_2\sqrt{\phi_1 + E^2} + \sigma^2 B_5 l_1 - B_6 5\sigma l_1\sqrt{\phi_1 + E^2} - \sigma^2 B_6 l_2;$$

$$r_7 = B_5\sigma l_2\sqrt{\phi_1 + E^2} + \sigma^2 B_6 l_1 + B_6\sigma l_1\sqrt{\phi_1 + E^2} + \sigma^2 B_5 l_2;$$

$$r_8 = B_5\sigma l_2\sqrt{\phi_1 + E^2} + \sigma^2 B_6 l_1 - B_6\sigma l_1\sqrt{\phi_1 + E^2} - \sigma^2 B_5 l_2;$$

$$r_9 = 2\sigma^2 B_5^2 l_3; \qquad r_{10} = 2\sigma^2 B_6^2 l_3; \qquad r_{11} = 2\sigma^2 l_1 l_3; \qquad r_{12} = 2\sigma^2 l_2 l_3;$$

$$r_{13} = \frac{2\sigma^2 l_3 + l_2^2(\phi_1 + E^2) + \sigma^2 l_1^2 - l_1(\phi_1 + E^2) - \sigma^2 l_2^2}{2};$$

$$r_{14} = \frac{-r_1}{4\sigma^2 - (\phi_1 + E^2)}; \quad r_{15} = \frac{-r_2}{4\sigma^2 - (\phi_1 + E^2)}; \quad r_{16} = \frac{-r_3}{3(\phi_1 + E^2)};$$

$$r_{17} = \frac{-r_4}{3(\phi_1 + E^2)}; \quad r_{18} = \frac{-r_5}{\sigma^2 + 2\sigma\sqrt{\phi_1 + E^2}}; \quad r_{19} = \frac{-r_7}{\sigma^2 + 2\sigma\sqrt{\phi_1 + E^2}};$$

$$r_{20} = \frac{-r_6}{\sigma^2 - 2\sigma\sqrt{\phi_1 + E^2}}; \quad r_{21} = \frac{-r_8}{\sigma^2 - 2\sigma\sqrt{\phi_1 + E^2}}; \quad r_{22} = \frac{-r_9}{\sigma^2 - (\phi_1 + E^2)};$$

$$r_{23} = \frac{-r_{10}}{\sigma^2 - (\phi_1 + E^2)}; \quad r_{24} = \frac{-r_{12}}{2\sqrt{\phi_1 + E^2}}; \quad r_{25} = \frac{-r_{11}}{2\sqrt{\phi_1 + E^2}}; \quad r_{26} = \frac{-r_{13}}{(\phi_1 + E^2)}.$$

Heat generation case.

$$A_1 = \frac{\mathrm{Gr}}{\mathrm{Re}}; \qquad A_2 = \frac{\mathrm{Gr}\, bmnh^2}{\mathrm{Re}}; \qquad A_3 = \sigma^2 h^2 k; \quad A_4 = mh^2 P;$$

$$A_5 = E^2 h^2 K; \qquad A_6 = \frac{K}{m}; \qquad A_7 = K\sigma^2 h^2 \frac{K}{m};$$

$$B_1 = \frac{1 - B_2 \sin\sqrt{\phi_1 - E^2}}{\cos\sqrt{\phi_1 - E^2}}; \qquad B_3 = \frac{1 - B_2 \sin\sqrt{\phi_1 - E^2}}{\cos\sqrt{\phi_1 - E^2}};$$

$$B_2 = \frac{\sqrt{\phi_2 - A_5}\cos\sqrt{\phi_2 - A_5}}{\sqrt{\phi_2 - A_5}\sin\sqrt{\phi_1 - E^2}\cos\sqrt{\phi_2 - A_5} + Kh\sqrt{\phi_1 - E^2}\cos\sqrt{\phi_1 - E^2}\sin\sqrt{\phi_2 - A_5}};$$

$$B_4 = \frac{B_3\cosh\sqrt{\phi_2 - A_5}}{\sinh\sqrt{\phi_2 - A_5}}; \qquad B_5 = \frac{D_1 - B_6 e^{-\sigma}}{e^{\sigma}};$$

$$B_6 = \frac{D_5\sqrt{A_3}\left(1+e^{-2\sqrt{A_3}}\right) - D_6\left(1-e^{-2\sqrt{A_3}}\right)}{\sqrt{A_3}\left(1-e^{-2\sigma}\right)\left(1+e^{-2\sqrt{A_3}}\right) + mh\sigma\left(1+e^{-2\sigma}\right)\left(1-e^{-2\sqrt{A_3}}\right)};$$

$$B_7 = \frac{-\left[mh\sigma\left(1+e^{-2\sigma}\right)D_5 + \left(1-e^{-2\sigma}\right)D_6\right]}{mh\sigma\left(1-e^{-2\sqrt{A_3}}\right)\left(1+e^{-2\sigma}\right) + \sqrt{A_3}\left(1+e^{-2\sqrt{A_3}}\right)\left(1-e^{-2\sigma}\right)};$$

$$B_8 = \frac{D_3 - B_7 e^{-\sqrt{A_3}}}{e^{\sqrt{A_3}}}; \qquad B_9 = \frac{D_7 - B_{10}\sin\sqrt{\phi_1 - E^2}}{\cos\sqrt{\phi_1 - E^2}};$$

$$B_{10} = \frac{\sqrt{\phi_2 - A_5}D_7\cosh\sqrt{\phi_2 - A_5} - \sqrt{\phi_2 - A_5}D_9\cos\sqrt{\phi_1 - E^2} + D_{10}\sin\sqrt{\phi_2 - A_5}\cos\sqrt{\phi_1 - E^2}}{\sqrt{\phi_2 - A_5}\sin\sqrt{\phi_1 - E^2}\cos\sqrt{\phi_2 - A_5} + Kh\sqrt{\phi_1 - E^2}\sin\sqrt{\phi_2 - A_5}\cos\sqrt{\phi_1 - E^2}}$$

$$+ \frac{-\sqrt{\phi_2 - A_5}D_8\cos\sqrt{\phi_2 - A_5}\cos\sqrt{\phi_1 - E^2}}{\sqrt{\phi_2 - A_5}\sin\sqrt{\phi_1 - E^2}\cos\sqrt{\phi_2 - A_5} + Kh\sqrt{\phi_1 - E^2}\sin\sqrt{\phi_2 - A_5}\cos\sqrt{\phi_1 - E^2}};$$

$$B_{11} = B_9 - D_8; \qquad B_{12} = \frac{B_{11}\cos\sqrt{\phi_2 - A_5} - D_9}{\sinh\sqrt{\phi_2 - A_5}}; \qquad B_{13} = \frac{D_{11} - B_{14}e^{-\sigma}}{e^{\sigma}};$$

$$B_{14} = \frac{D_{15}\sqrt{A_3}\left(1+e^{-2\sqrt{A_3}}\right) - D_{16}\left(1-e^{-2\sqrt{A_3}}\right)}{\sqrt{A_3}\left(1+e^{-2\sqrt{A_3}}\right)\left(1-e^{-2\sigma}\right) + mh\sigma\left(1+e^{-2\sigma}\right)\left(1-e^{-2\sqrt{A_3}}\right)};$$

$$B_{15} = \frac{-\left[D_{15}mh\sigma\left(1+e^{-2\sigma}\right) + D_{16}\left(1-e^{-2\sigma}\right)\right]}{mh\sigma\left(1+e^{-2\sigma}\right)\left(1-e^{-2\sqrt{A_3}}\right) + \sqrt{A_3}\left(1-e^{-2\sigma}\right)\left(1+e^{-2\sqrt{A_3}}\right)};$$

$$B_{16} = \frac{D_{13} - B_{15}e^{-\sqrt{A_3}}}{e^{\sqrt{A_3}}};$$

$$D_1 = -l_1\cos\sqrt{\phi_1 - E^2} - l_2\sin\sqrt{\phi_1 - E^2} - l_3; \quad D_2 = l_4 + l_6 - l_1 - l_3;$$

$$D_3 = -l_4\cos\sqrt{\phi_2 - A_5} + l_5\sin\sqrt{\phi_2 - A_5} - l_6; \quad D_4 = l_5\sqrt{\phi_2 - A_5} - mhl_2\sqrt{\phi_1 - E^2};$$

$$D_5 = D_2 - D_1e^{-\sigma} + D_3e^{-\sqrt{A_3}}; \quad D_6 = D_4 - mh\sigma D_1e^{-\sigma} - D_3\sqrt{A_3};$$

$$D_7 = -r_{14}\cos 2\sqrt{\phi_1 - E^2} - r_{15}\sin 2\sqrt{\phi_1 - E^2} - r_{16}e^{\sigma}\cos\sqrt{\phi_1 - E^2} - r_{17}e^{\sigma}\sin\sqrt{\phi_1 - E^2}$$

$$- r_{18}e^{-\sigma}\cos\sqrt{\phi_1 - E^2} - r_{19}e^{-\sigma}\sin\sqrt{\phi_1 - E^2} - r_{20}\cos\sqrt{\phi_1 - E^2}$$

$$- r_{21}\sin\sqrt{\phi_1 - E^2} - r_{22}e^{2\sigma} - r_{23}e^{-2\sigma} - r_{24}e^{\sigma} - r_{25}e^{-\sigma} - r_{26};$$

$$D_8 = g_{14} + g_{16} + g_{18} + g_{22} + g_{23} + g_{25} + g_{26} - r_{22} - r_{23} - r_{14} - r_{16} - r_{18} - r_{24} - r_{25} - r_{26};$$

$$D_9 = -g_{14}\cos 2\sqrt{\phi_2 - A_5} + g_{15}\sin 2\sqrt{\phi_2 - A_5} - g_{16}e^{-\sqrt{A_3}}\cos\sqrt{\phi_2 - A_5}$$
$$+g_{17}e^{-\sqrt{A_3}}\sin\sqrt{\phi_2 - A_5} - g_{18}e^{\sqrt{A_3}}\cos\sqrt{\phi_2 - A_5} + g_{19}e^{\sqrt{A_3}}\sin\sqrt{\phi_2 - A_5}$$
$$+g_{20}\cos\sqrt{\phi_2 - A_5} - g_{21}\sin\sqrt{\phi_2 - A_5} - g_{22}e^{-2\sqrt{A_3}} - g_{23}e^{2\sqrt{A_3}}$$
$$-g_{24}e^{-\sqrt{A_3}} - g_{25}e^{\sqrt{A_3}} + g_{26};$$

$$D_{10} = g_{22}2\sqrt{A_3} - 2\sqrt{A_3}\,g_{23} + 2\sqrt{\phi_2 - A_5}\,g_{15} + \sqrt{A_3}\,g_{16} - g_{18}\sqrt{A_3} + g_{17}\sqrt{\phi_2 - A_5}$$
$$+g_{19}\sqrt{\phi_2 - A_5} + g_{20} + g_{24}\sqrt{A_3} - g_{25}\sqrt{A_3} - 2Kh\sigma r_{22} + 2Kh\sigma r_{15}$$
$$-2Kh\sqrt{\phi_1 - E^2}\,r_{15} - r_{16}Kh\sigma + r_{18}Kh\sigma - Khr_{17}\sqrt{\phi_1 - E^2}$$
$$-Khr_{19}\sqrt{\phi_1 - E^2} - r_{20}Kh - Kh\sigma r_{24} + Kh\sigma r_{25};$$

$$D_{11} = -l_9\cos\sqrt{\phi_1 - E^2} - l_{10}\sin\sqrt{\phi_1 - E^2} - l_{19}e^{2\sigma} + l_{20}e^{-2\sigma} + l_7\cos 2\sqrt{\phi_1 - E^2}$$
$$-l_8\sin 2\sqrt{\phi_1 - E^2} - l_{11}e^{\sigma}\cos\sqrt{\phi_1 - E^2} - l_{13}e^{-\sigma}\cos\sqrt{\phi_1 - E^2}$$
$$-l_{12}e^{\sigma}\sin\sqrt{\phi_1 - E^2} - l_{14}e^{-\sigma}\sin\sqrt{\phi_1 - E^2} - l_{16}\sin\sqrt{\phi_1 - E^2}$$
$$-l_{15}\cos\sqrt{\phi_1 - E^2} - l_{17}e^{\sigma} - l_{18}e^{-\sigma} - l_{21};$$

$$D_{12} = l_{24} + l_{22} + l_{26} + l_{28} + l_{32} + l_{33} + l_{36} - l_9 - l_{19} - l_{20} - l_7 - l_{11} - l_{13} - l_{21};$$

$$D_{13} = -l_{24}\cos\sqrt{\phi_2 - A_5} + l_{25}\sin\sqrt{\phi_2 - A_5} - l_{22}\cos 2\sqrt{\phi_2 - A_5} + l_{23}\sin 2\sqrt{\phi_2 - A_5}$$
$$+l_{27}e^{-\sqrt{A_3}}\sin\sqrt{\phi_2 - A_5} + l_{29}e^{\sqrt{A_3}}\sin\sqrt{\phi_2 - A_5} - l_{26}e^{-\sqrt{A_3}}\cos\sqrt{\phi_2 - A_5}$$
$$-l_{28}e^{\sqrt{A_3}}\cos\sqrt{\phi_2 - A_5} + l_{30}\cos\sqrt{\phi_2 - A_5} - l_{31}\sin\sqrt{\phi_2 - A_5}$$
$$-l_{32}e^{-2\sqrt{A_3}} - l_{33}e^{2\sqrt{A_3}} + l_{34}e^{-\sqrt{A_3}} + l_{35}e^{\sqrt{A_3}} + l_{36};$$

$$D_{14} = l_{25}\sqrt{\phi_2 - A_5} + 2l_{23}\sqrt{\phi_2 - A_5} + l_{27}\sqrt{\phi_2 - A_5} + l_{29}\sqrt{\phi_2 - A_5} + l_{26}\sqrt{A_3}$$
$$-l_{28}\sqrt{A_3} + l_{30} + 2l_{32}\sqrt{A_3} - 2l_{33}\sqrt{A_3} + l_{34} + l_{35} - mhl_{10}\sqrt{\phi_1 - E^2}$$
$$-2mh\sigma l_{19} + 2mh\sigma l_{20} - 2mh\sqrt{\phi_1 - E^2}\,l_8 - mh\sigma l_{11} + mh\sigma l_{13}$$
$$-mh\sqrt{\phi_1 - E^2}\,l_{12} - mh\sqrt{\phi_1 - E^2}\,l_{14} - mhl_{15} - mhl_{17} - mhl_{18};$$

$$D_{15} = D_{12} - D_{11}e^{-\sigma}D_{13}e^{-\sqrt{A_3}}; \qquad D_{16} = D_{14} - mh\sigma D_{11}e^{-\sigma} - D_{13}\sqrt{A_3}e^{-\sqrt{A_3}};$$

$$g_1 = B_7^2(A_6A_3 + A_7); \qquad g_2 = B_8^2(A_6A_3 + A_7); \qquad g_4 = A_7l_4l_5 - A_6l_4l_5(\phi_2 - A_5);$$

$$g_3 = \frac{A_6l_5^2(\phi_2 - A_5) - A_6l_4^2(\phi_2 - A_5) + A_7l_4^2 - A_7l_5^2}{2};$$

$$g_5 = 2\left(A_6l_5\sqrt{\phi_2 - A_5}B_7\sqrt{A_3} + A_7B_7l_4\right); \quad g_6 = 2\left(A_7B_8l_4 - A_6B_8l_5\sqrt{\phi_2 - A_5}\sqrt{A_3}\right);$$

$$g_7 = 2\left(A_7B_7l_5 - A_6B_7l_4\sqrt{\phi_2 - A_5}\sqrt{A_3}\right);$$

$$g_8 = 2\left(A_7B_8l_5 + A_6B_8l_4\sqrt{\phi_2 - A_5}\sqrt{A_3}\right);$$

$$g_9 = 2A_7l_4l_6; \qquad g_{10} = 2A_7l_5l_6; \qquad g_{11} = 2A_7B_7l_6; \qquad g_{12} = 2A_7B_8l_6;$$

$$g_{13} = 2A_7l_6^2 + \frac{1}{2}A_6l_5^2(\phi_2 - A_5) + \frac{1}{2}A_6l_5^2(\phi_2 - A_5) - 2A_6A_3B_7B_8 + \frac{1}{2}A_7l_4^2 + \frac{1}{2}A_7l_5^2 + 2A_7B_7B_8;$$

$$g_{14} = \frac{g_3}{3(\phi_2 - A_5)}; \qquad g_{15} = \frac{g_4}{3(\phi_2 - A_5)};$$

$$g_{16} = \frac{2\sqrt{A_3}\sqrt{\phi_2 - A_5}\,g_7}{A_3^2 + 4A_3(\phi_2 - A_5)} - \frac{g_5}{A_3 + 4(\phi_2 - A_5)};$$

$$g_{17} = \frac{2\sqrt{A_3}\sqrt{\phi_2 - A_5}\,g_5}{A_3^2 + 4A_3(\phi_2 - A_5)} + \frac{g_7}{A_3 + 4(\phi_2 - A_5)};$$

$$g_{18} = \frac{2\sqrt{A_3}\sqrt{\phi_2 - A_5}\,g_8}{A_3^2 + 4A_3(\phi_2 - A_5)} + \frac{g_6}{A_3 + 4(\phi_2 - A_5)};$$

$$g_{19} = \frac{2\sqrt{A_3}\sqrt{\phi_2 - A_5}\,g_6}{A_3^2 + 4A_3(\phi_2 - A_5)} - \frac{g_8}{A_3 + 4(\phi_2 - A_5)};$$

$$g_{20} = \frac{g_{10}}{2\sqrt{\phi_2 - A_5}}; \qquad g_{21} = \frac{-g_9}{2\sqrt{\phi_2 - A_5}}; \qquad g_{22} = \frac{-g_9}{A_3 - (\phi_2 - A_5)};$$

$$g_{23} = \frac{-g_{10}}{A_3 - (\phi_2 - A_5)}; \qquad g_{24} = \frac{-g_{11}}{A_3 + (\phi_2 - A_5)};$$

$$g_{25} = \frac{-g_{12}}{A_3 + (\phi_2 - A_5)}; \qquad g_{26} = \frac{-g_{13}}{\phi_2 - A_5};$$

$$l_1 = \frac{-A_1B_1}{(\phi_1 - E^2) + \sigma^2}; \qquad l_2 = \frac{-A_2B_2}{(\phi_1 - E^2) + \sigma^2}; \qquad l_3 = \frac{-P}{\sigma^2};$$

$$l_4 = \frac{-A_2B_3}{(\phi_2 - A_5) + A_3}; \qquad l_5 = \frac{-A_5B_4}{(\phi_2 - A_5) + A_3}; \qquad l_6 = \frac{-A_4}{A_3};$$

$$l_7 = \frac{A_1r_{14}}{4(\phi_1 - E^2) + \sigma^2}; \qquad l_8 = \frac{A_1r_{15}}{4(\phi_1 - E^2) + \sigma^2};$$

$$l_9 = \frac{2A_1\sqrt{\phi_1 - E^2}\, r_{21}}{\left[(\phi_1 - E^2) + \sigma^2\right]^2} + \frac{A_1 B_9}{(\phi_1 - E^2) + \sigma^2}\,;$$

$$l_{10} = \frac{-2A_1\sqrt{\phi_1 - E^2}\, r_{20}}{\left[(\phi_1 - E^2) + \sigma^2\right]^2} + \frac{A_1 B_{10}}{(\phi_1 - E^2) + \sigma^2}\,;$$

$$l_{11} = \frac{A_1 r_{16}}{(\phi_1 - E^2) + 4\sigma^2} + \frac{2A_1\sigma r_{15}}{(\phi_1 - E^2)^{3/2} + 4\sigma^2\sqrt{\phi_1 - E^2}}\,;$$

$$l_{12} = \frac{A_1 r_{17}}{(\phi_1 - E^2) + 4\sigma^2} - \frac{2A_1\sigma r_{16}}{(\phi_1 - E^2)^{3/2} + 4\sigma^2\sqrt{\phi_1 - E^2}}\,;$$

$$l_{13} = \frac{A_1 r_{18}}{(\phi_1 - E^2) + 4\sigma^2} - \frac{2A_1\sigma r_{19}}{(\phi_1 - E^2)^{3/2} + 4\sigma^2\sqrt{\phi_1 - E^2}}\,;$$

$$l_{14} = \frac{A_1 r_{19}}{(\phi_1 - E^2) + 4\sigma^2} + \frac{2A_1\sigma r_{18}}{(\phi_1 - E^2)^{3/2} + 4\sigma^2\sqrt{\phi_1 - E^2}}\,;$$

$$l_{15} = \frac{A_1 r_{20}}{(\phi_1 - E^2) + \sigma^2}\,; \qquad l_{16} = \frac{A_1 r_{21}}{(\phi_1 - E^2) + \sigma^2}\,; \qquad l_{17} = \frac{-A_1 r_{24}}{2\sigma}\,;$$

$$l_{18} = \frac{-A_1 r_{25}}{2\sigma}\,; \qquad l_{19} = \frac{-A_1 r_{22}}{3\sigma^2}\,; \qquad l_{20} = \frac{-A_1 r_{23}}{3\sigma^2}\,; \qquad l_{21} = \frac{A_1 r_{26}}{\sigma^2}\,;$$

$$l_{22} = \frac{A_2 g_{14}}{A_3 + 4(\phi_2 - A_5)}\,; \qquad l_{23} = \frac{A_2 g_{15}}{A_3 + 4(\phi_2 - A_5)}\,;$$

$$l_{24} = \frac{A_2 B_{11}\left[A_3 + (\phi_2 - A_5) + 2A_2\sqrt{\phi_2 - A_5}\, g_{21}\right]}{\left[A_3 + (\phi_2 - A_5)\right]^2}\,; \quad l_{26} = \frac{A_2 g_{16}\sqrt{\phi_2 - A_5} + 2\sqrt{A_3}\, A_2 g_{17}}{\sqrt{\phi_2 - A_5}\left[4A_3 + (\phi_2 - A_5)\right]}\,;$$

$$l_{25} = \frac{A_2 B_{12}\left[A_3 + (\phi_2 - A_5) + 2A_2\sqrt{\phi_2 - A_5}\, g_{20}\right]}{\left[A_3 + (\phi_2 - A_5)\right]^2}\,; \quad l_{27} = \frac{A_2 g_{17}\sqrt{\phi_2 - A_5} - 2\sqrt{A_3}\, A_2 g_{16}}{\sqrt{\phi_2 - A_5}\left[4A_3 + (\phi_2 - A_5)\right]}\,;$$

$$l_{28} = \frac{A_2 g_{18}\sqrt{\phi_2 - A_5} - 2\sqrt{A_3}\, A_2 g_{19}}{\sqrt{\phi_2 - A_5}\left[4A_3 + (\phi_2 - A_5)\right]}\,; \qquad l_{29} = \frac{A_2 g_{19}\sqrt{\phi_2 - A_5} + 2\sqrt{A_3}\, A_2 g_{18}}{\sqrt{\phi_2 - A_5}\left[4A_3 + (\phi_2 - A_5)\right]}\,;$$

$$l_{30} = \frac{A_2 g_{20}}{(\phi_2 - A_5) + A_3}\,; \qquad l_{31} = \frac{A_2 g_{21}}{(\phi_2 - A_5) + A_3}\,; \qquad l_{32} = \frac{-A_2 g_{22}}{3A_3}\,;$$

$$l_{33} = \frac{-A_2 g_{23}}{3A_3}\,; \qquad l_{34} = \frac{-A_2 g_{24}}{3\sqrt{A_3}}\,; \qquad l_{35} = \frac{-A_2 g_{25}}{(\phi_2 + A_5) - A_3}\,; \qquad l_{36} = \frac{A_2 g_{26}}{A_3}\,;$$

$$P_1 = \sqrt{\phi_1 - E^2}\,; \qquad P_2 = \sqrt{\phi_2 - A_5}\,;$$

$$r_1 = 2\sigma^2 B_5^2; \qquad r_2 = 2\sigma^2 B_6^2;$$

$$r_4 = l_1 l_2\left[\sigma^2 - (\phi_1 - E^2)\right]; \qquad r_3 = \frac{(l_2^2 - l_1^2)\left[(\phi_1 - E^2) - \sigma^2\right]}{2}\,;$$

$$r_5 = 2\left(B_5\sigma\, l_2\sqrt{\phi_1 - E^2} + \sigma^2\, B_5 l_1\right); \qquad r_6 = 2\left(-B_6\sigma\, l_2\sqrt{\phi_1 - E^2} + \sigma^2\, B_6 l_1\right);$$

$$r_7 = 2\left(-B_5\sigma\, l_1\sqrt{\phi_1 - E^2} + \sigma^2\, B_5 l_2\right); \qquad r_8 = 2\left(B_6\sigma\, l_1\sqrt{\phi_1 - E^2} + \sigma^2\, B_6 l_2\right);$$

$$r_9 = 2\sigma^2 l_1 l_3; \qquad r_{10} = 2\sigma^2 l_2 l_3; \qquad r_{11} = 2\sigma^2 B_5 l_3; \qquad r_{12} = 2\sigma^2 B_6 l_3;$$

$$r_{13} = \frac{2\sigma^2 l_3^2 + l_2^2(\phi_1 - E^2) + \sigma^2 l_1^2 + l_1^2(\phi_1 - E^2) + \sigma^2 l_2^2}{2};$$

$$r_{14} = \frac{r_3}{3(\phi_1 - E^2)}; \qquad r_{15} = \frac{-r_2}{4\sigma^2 - (\phi_1 - E^2)};$$

$$r_{16} = \frac{2\sigma\sqrt{\phi_1 - E^2}\, r_7}{\sigma^4 + 4\sigma^2(\phi_1 - E^2)} - \frac{r_5}{\sigma^2 + 4(\phi_1 - E^2)};$$

$$r_{17} = \frac{2\sigma\sqrt{\phi_1 - E^2}\, r_5}{\sigma^4 + 4\sigma^2(\phi_1 - E^2)} - \frac{r_7}{\sigma^2 + 4(\phi_1 - E^2)};$$

$$r_{18} = \frac{-2\sigma\sqrt{\phi_1 - E^2}\, r_8}{\sigma^4 + 4\sigma^2(\phi_1 - E^2)} - \frac{r_6}{\sigma^2 + 4(\phi_1 - E^2)};$$

$$r_{19} = \frac{2\sigma\sqrt{\phi_1 - E^2}\, r_6}{\sigma^4 + 4\sigma^2(\phi_1 - E^2)} - \frac{r_8}{\sigma^2 + 4(\phi_1 - E^2)};$$

$$r_{20} = \frac{r_{10}}{2\sqrt{\phi_1 - E^2}}; \qquad r_{21} = \frac{-r_9}{2\sqrt{\phi_1 - E^2}};$$

$$r_{22} = \frac{-r_1}{4\sigma^2 + (\phi_1 - E^2)}; \qquad r_{23} = \frac{-r_2}{4\sigma^2 + (\phi_1 - E^2)};$$

$$r_{24} = \frac{-r_{11}}{\sigma^2 + (\phi_1 - E^2)}; \qquad r_{25} = \frac{-r_{12}}{\sigma^2 + (\phi_1 - E^2)};$$

$$r_{26} = \frac{-r_{13}}{\phi_1 - E^2}.$$

□◆◆◆□